NASA/TM-2009-215564

An Overview of the State of the Art in Atomistic and Multiscale Simulation of Fracture

Erik Saether
Langley Research Center, Hampton, Virginia

Vesselin Yamakov
National Institute of Aerospace, Hampton, Virginia

Dawn R. Phillips
Lockheed Martin Space Operations, Hampton, Virginia

Edward H. Glaessgen
Langley Research Center, Hampton, Virginia

February 2009

NASA STI Program . . . in Profile

Since its founding, NASA has been dedicated to the advancement of aeronautics and space science. The NASA scientific and technical information (STI) program plays a key part in helping NASA maintain this important role.

The NASA STI program operates under the auspices of the Agency Chief Information Officer. It collects, organizes, provides for archiving, and disseminates NASA's STI. The NASA STI program provides access to the NASA Aeronautics and Space Database and its public interface, the NASA Technical Report Server, thus providing one of the largest collections of aeronautical and space science STI in the world. Results are published in both non-NASA channels and by NASA in the NASA STI Report Series, which includes the following report types:

- TECHNICAL PUBLICATION. Reports of completed research or a major significant phase of research that present the results of NASA programs and include extensive data or theoretical analysis. Includes compilations of significant scientific and technical data and information deemed to be of continuing reference value. NASA counterpart of peer-reviewed formal professional papers, but having less stringent limitations on manuscript length and extent of graphic presentations.

- TECHNICAL MEMORANDUM. Scientific and technical findings that are preliminary or of specialized interest, e.g., quick release reports, working papers, and bibliographies that contain minimal annotation. Does not contain extensive analysis.

- CONTRACTOR REPORT. Scientific and technical findings by NASA-sponsored contractors and grantees.

- CONFERENCE PUBLICATION. Collected papers from scientific and technical conferences, symposia, seminars, or other meetings sponsored or co-sponsored by NASA.

- SPECIAL PUBLICATION. Scientific, technical, or historical information from NASA programs, projects, and missions, often concerned with subjects having substantial public interest.

- TECHNICAL TRANSLATION. English-language translations of foreign scientific and technical material pertinent to NASA's mission.

Specialized services also include creating custom thesauri, building customized databases, and organizing and publishing research results.

For more information about the NASA STI program, see the following:

- Access the NASA STI program home page at *http://www.sti.nasa.gov*

- E-mail your question via the Internet to help@sti.nasa.gov

- Fax your question to the NASA STI Help Desk at 443-757-5803

- Phone the NASA STI Help Desk at 443-757-5802

- Write to:
  NASA STI Help Desk
  NASA Center for AeroSpace Information
  7115 Standard Drive
  Hanover, MD 21076-1320

NASA/TM-2009-215564

An Overview of the State of the Art in Atomistic and Multiscale Simulation of Fracture

Erik Saether
Langley Research Center, Hampton, Virginia

Vesselin Yamakov
National Institute of Aerospace, Hampton, Virginia

Dawn R. Phillips
Lockheed Martin Space Operations, Hampton, Virginia

Edward H. Glaessgen
Langley Research Center, Hampton, Virginia

National Aeronautics and
Space Administration

Langley Research Center
Hampton, Virginia 23681-2199

February 2009

Available from:

NASA Center for AeroSpace Information
7115 Standard Drive
Hanover, MD 21076-1320
443-757-5802

Table of Contents

1. Introduction 1
2. Atomistic Simulations of Fracture at Interfaces 2
2.1 Historical Development 2
2.2 Problematic Issues in the Atomistic Simulations 6
2.2.1 Overcoming Length Scale Limitations 7
2.2.2 Overcoming Time Scale Limitations 9
2.2.3 Interatomic Potentials 11
3. Introduction to Multiscale Methods 13
3.1 Classification of Multiscale Approaches 14
3.2 Concurrent Multiscale Methods 16
3.2.1 The Macroscopic, Atomistic, Ab initio Dynamics Method 16
3.2.2 The Finite Element-Atomistic Method 17
3.2.3 The Coarse Grained Molecular Dynamics Method 18
3.2.4 The Quasicontinuum Method 19
3.2.5 The Bridging Domain Method 21
3.2.6 The Coupled Atomistic/Discrete Dislocation Method 21
3.2.7 The Equivalent Continuum Model 24
3.2.8 The Embedded Statistical Coupling Method 25
3.2.9 Issues in the Development of Concurrent Methods 26
3.3 Sequential Multiscale Methods 27
3.3.1 Cohesive Zone Models 27
3.3.1.1 Mixed-Mode Representation using CZMs 32
3.3.1.2 CZM Models for Interfacial Sliding 37
3.3.2 Nanoscopic Length-Scale Coupling Through CZMs 39
3.3.3 Decohesion Finite Element Formulations 45

4. Summary 49
5. References 51

Abstract

The emerging field of nanomechanics is providing a new focus in the study of the mechanics of materials, particularly in simulating fundamental atomic mechanisms involved in the initiation and evolution of damage. Simulating fundamental material processes using first principles in physics strongly motivates the formulation of computational multiscale methods to link macroscopic failure to the underlying atomic processes from which all material behavior originates. This report gives an overview of the state of the art of the atomistic simulation of fracture and the application of concurrent and sequential multiscale methods to analyze damage and failure mechanisms across length scales.

1.0 Introduction

Classical fracture mechanics is based on a continuum description of material domains and fracture behavior described in terms of empirical parameters (K_{IC}, J-R curves, Crack Tip Opening Angle, etc.). The emerging field of nanomechanics is providing a new insight into fracture processes beyond that available in continuum mechanics by simulating and characterizing fundamental atomic mechanisms involved in the initiation and evolution of damage. These mechanisms occur at length scales on the order of 10^{-10} to 10^{-3} m and include those leading to the creation of traction-free surfaces (e.g., atomic bond breakage) and plastic defects (e.g., dislocations, twins, stacking faults).

At length scales below 10^{-6} m, direct observations of damage processes are extremely difficult to obtain, thus atomistic simulations have proven to be an invaluable tool for understanding the fundamental processes of fracture. Either quantum mechanics (ab-initio, tight-binding (TB) or density-functional theory (DFT)) methods or classical molecular dynamics (MD) or molecular statics (MS) methods can be used to simulate fundamental material processes using *first principles* in physics and provide an ultimate

understanding of deformation and fracture processes at the atomistic level. These predictions of material behavior at nanometer length scales promise the development of physics-based "bottom-up" multiscale analyses that can aid in understanding the evolution of failure mechanisms across length scales.

This report is intended to give an overview of the state of the art in the atomistic simulation of fracture and the application of concurrent and sequential multiscale methods to analyze damage and failure mechanisms across length scales.

2.0 Atomistic Simulations of Fracture at Interfaces

Atomistic simulations in material science have a continuously increasing role in understanding the fundamental physics-based mechanisms of material behavior. The rapid growth of computational power and the continuous development of more robust and more efficient numerical methods have resulted in a substantial improvement in the accuracy and the performance of simulation models. Two decades ago (ca. 1980s), atomistic simulations were mostly used in qualitative predictions of material behavior (e.g., phase transitions of Lennard-Jones metallic systems, Ising model calculations in ferromagnetic crystals, Random Walk models for polymer chains). Currently (ca. 2008), it is possible to quantitatively predict many of the properties of a specific material with a given structural and chemical composition. The success of the transition from qualitative to quantitative predictions has made possible the development of new "bottom-up" approaches in modeling the mechanical properties of materials starting from the basic atomic level interactions. In these approaches, atomistic simulations play a key role in providing the basic information from the underlying atomistic processes that ultimately govern the macroscopic material parameters.

2.1 Historical Development

MD simulations are invaluable in studying fracture of interfaces, such as grain boundaries in metals, where continuum mechanics can not adequately represent structural

inhomogeneity. To illustrate the historical application of MD simulations to the study of fracture, selected analyses presented in the literature will be discussed.

Some of the first attempts to qualitatively model the statics and dynamics of fracture at an atomic level date back to 1976 when Ashurst and Hoover (Ashurst and Hoover, 1976) used a two-dimensional triangular lattice of 512 mass points interacting with linear-force Hooke's-law springs as a representative model for a crystal (Figure 1). The system was evolved in a molecular-dynamics (MD) sense, through integrating Newton's equations of motion for each mass point. The forces between the mass points were defined as linear functions of the point displacements up to a maximum strain of 10% at which time the force was set to zero, representing bond breaking. Even for this simplest crystal model, the results exhibitied a number of interesting physical phenomena, such as varying crack propagation velocity and widespread damage around the crack tip, revealing details that can not be predicted using continuum mechanics.

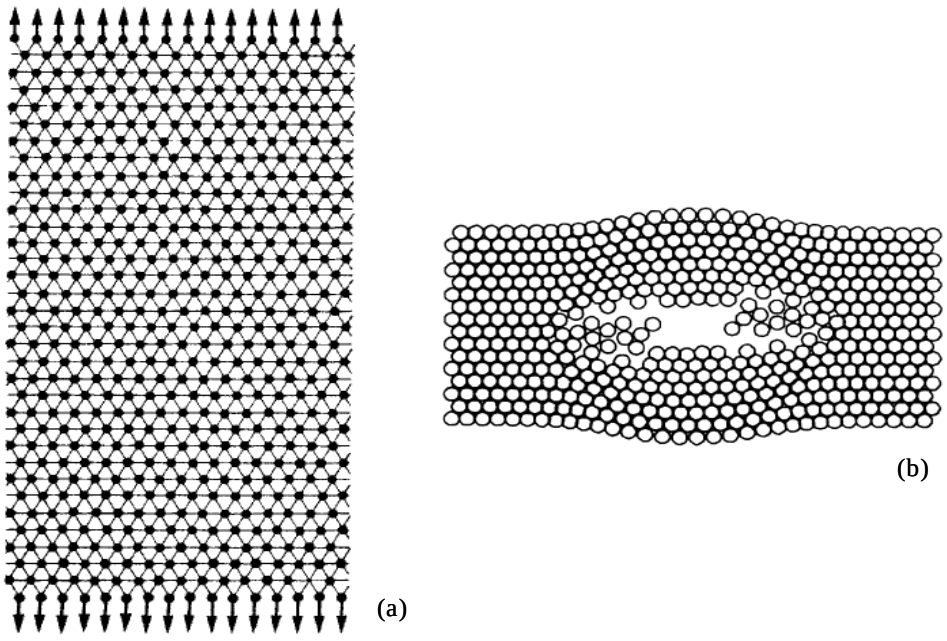

Figure 1. (a) Two-dimensional triangular lattice of 512 mass points interacting with linear-force Hooke's-law springs as a representative model for a crystal; (b) Image of a nanocrack nucleated due to atomic bond breaking in the triangular two-dimensional lattice. (From Ashurst and Hoover, 1976)

An early attempt to qualitatively simulate grain boundary segregation through crack propagation by MD was reported by Ishida et al. (1984) with the simulation of fracture in iron. These were the first simulations to reveal physical mechanisms of plastic processes, such as dislocation nucleation, developing at the crack tip.

A pioneering systematic MD analysis relating the crystallography of a large set of tilt and twist grain boundaries in Cu and Au to their grain boundary (GB) energy, E^{GB}, and cleavage properties was performed by Wolf some years later (Wolf, 1990). In this study, a large representative set of symmetric GBs in a two-dimensional space of the two characteristic parameters, the twist (φ) and tilt (θ) angle, were investigated and their cleavage energies, E^{cl}, were estimated. Cleavage energy is defined by an extension to the Griffith criteria for crack growth given by

$$E^{cl} = 2\gamma - E^{GB} \tag{1}$$

where γ is the surface energy of the GB plane. Thus, a structure-energy correlation for all symmetric GBs in an fcc metal was derived and related to the inter-granular fracture properties. In a related study, Yip and Wolf (Yip and Wolf, 1989) evaluated the atomistic concept for simulation of GB fracture. They presented an integrated approach for the study of the correlation between crystallographical and chemical interfacial structure and the physical properties relevant to intergranular fracture. This approach included the use of four related techniques: lattice statics for the determination of grain boundary energies; lattice dynamics for the analysis of local elastic constants; Monte Carlo simulation for determining solute segregation in grain boundary structure; and molecular dynamics simulation for modeling dynamic crack propagation. The major implication of these early works is that the problem of GB fracture must be considered from the point of view of the structure and properties of the GB, which significantly affect the process of crack propagation.

More recent MD simulation studies have exploited various aspects of the inter-granular crack propagation process. These include studies on the decohesion strength of a GB and its dependence on impurities (Golubovic et al., 1995; Grujicic et al., 1997; Gumbsch, 1999); fracture stress and strain of the GB interface as a function of the atomic disorder due to the presence of vacancies and interstitials (Heino et al., 1998); dislocation emission from the crack tip as a function of the GB crystallography and structure (Hoagland, 1997; Cleri et al., 1999; Farkas, 2000); and crack propagation in nanocrystalline metals (Farkas et al., 2002; Rudd and Belak, 2002).

Advances in computational technology have already made simulations of crack behavior in a single crystal of 10^8 atoms (Abraham, 1997; Zhou et al., 1997; Abraham, 2001; Bulatov et al. 1998) or even 10^9 atoms (Abraham et al., 2002) possible (Figure 2).

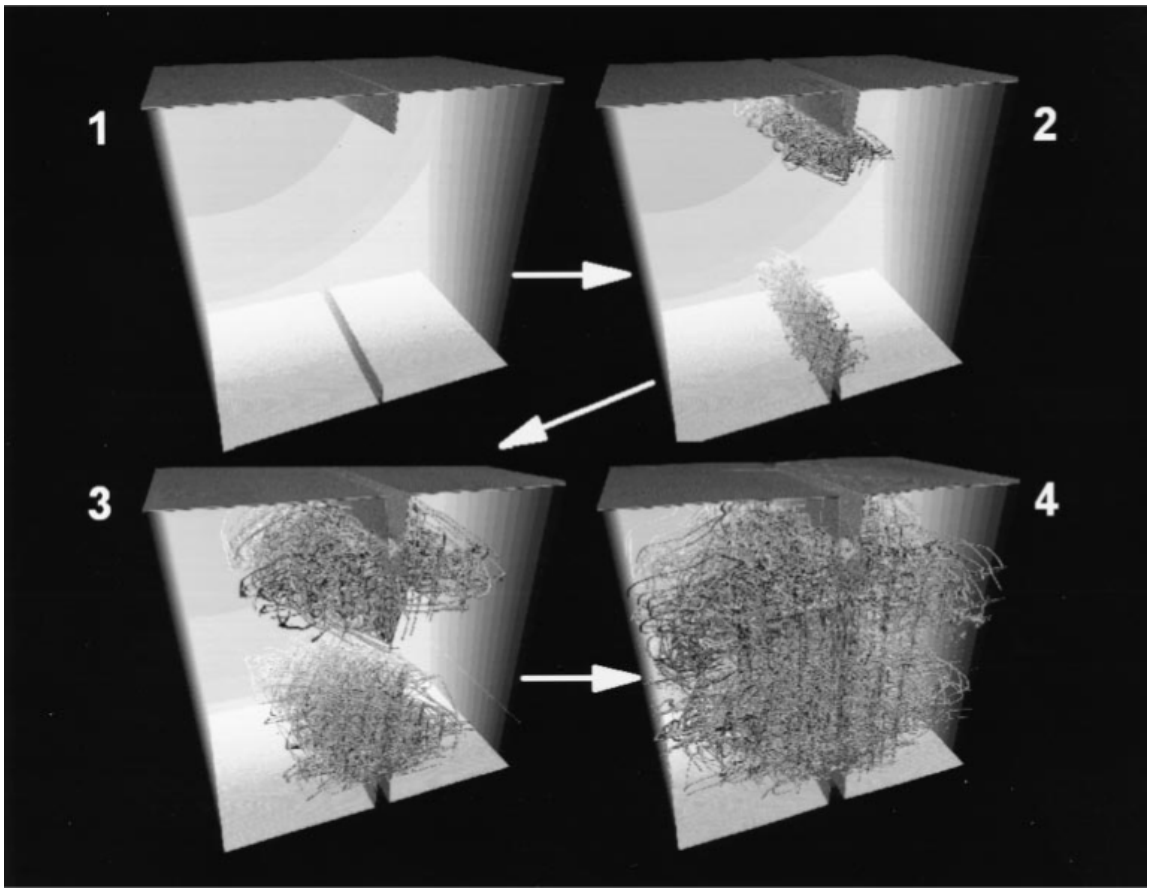

Figure 2. A billion atom molecular-dynamics simulation of a crack growing in a single crystal of Cu. Intensive emissions of dislocations from the crack tips are observed. (From Abraham et al., 2002)

Although they remain impractical for systematic studies, or for use by most practitioners, these large scale atomistic simulations are able to reveal many of the complex processes taking place at the crack tip, including dislocation emission and crack blunting in a three-dimensional environment. The atomistic simulations approach length scales where gradient theories of continuum mechanics (on the order of 0.1 μm) become valid, that is, where the discrete atomic structure of the matter starts to be smoothed out. In this way, length scales of the atomistic simulations have begun to overlap those of continuum model simulations (Bulatov et al., 1998; Cleri et al., 1998), using, for example, the finite-element method (FEM) (Xu and Needleman, 1994) or dislocation dynamics simulation (Noronha and Farkas, 2002) techniques. Still, computational demands and differing mechanistic paradigms give rise to various issues and limitations in pure atomistic simulation.

2.2 Problematic Issues in the Atomistic Simulations

The ability of the atomistic computer simulations to predict every atom's position and velocity at any moment in time provides valuable information on fundamental material behavior not accessible from experiments. However, the necessity of representing the material atom by atom introduces several major issues that must be addressed. First is the issue of the extremely small length-scale, typically less than 100 nm, which may make the system behavior a strong function of its boundary conditions. Second is the issue of the short timescale, of the order of pico and nanoseconds. For example, billion atom atomistic simulations remain severely limited in time scale; even the most powerful current supercomputers available today (ca. 2008) can not simulate the system response beyond the nanosecond range. This short timescale prevents the studies of low-rate or low-temperature deformation processes, such as diffusion or migration of defects and structural changes that take place over longer time scales. Third is the issue of the accuracy of the available interatomic potential functions used in the atomistic simulations to define the interactions between individual atoms. These potential functions define the overall physical properties of the simulated material so their accuracy is crucial for the correct representation of the system behavior.

2.2.1 Overcoming Length Scale Limitations

There are a number of methods suggested in the literature to overcome the length scale limitations. All of them rely on defining special types of boundary conditions that may aid in mimicking an infinite system. The most popular is the use of periodic boundary conditions (PBC). In a system modeled using PBCs (Allan and Tildesley, 1989), atoms at the boundary are made to interact with the atoms on the opposite side of the system as if the system has been multiplied in space. In this way, the boundary atoms are placed in the same surrounding environment as the interior atoms. The system, while remaining finite in volume, effectively has no boundaries. The PBC method works very well when the correlation length (the length over which one event can affect another event) of the system is smaller than the system size. If this is not true, the correlation effects are extended beyond the system size and are periodically multiplied causing severe artifacts such as strong distortions of the elastic fields or correlated dynamic oscillations in the system. Processes that produce long-range stress-strain fields, including cracks, exhibit these artifacts, and may be poorly handled by PBCs.

For the case of long range elastic fields, another type of boundary condition, called a “flexible” or “elastic” boundary condition (EBC) has been developed (Sinclair et al., 1978). In a system modeled using EBCs, the elastic strain field due to a simulated defect in the system, such as a dislocation or a crack, is calculated analytically under infinite boundary conditions. The resulting displacements calculated at the simulated system boundary are applied by fixing the boundary atoms at precalculated displaced positions. In this way, the boundary atoms mimic the strain field of an infinite continuum. The method was commonly used for studying the structure of dislocation cores and the processes of dislocation core interactions. EBCs were also widely used for crack simulations.

The drawback of the EBC method is that an imposed constraint on the boundary atoms affects the dynamics and the thermodynamics of the system. In addition, the precalculated atomic displacements are valid only for the initial configuration of the

system. As the system evolves in time, these boundary displacements increasingly deviate from the actual stress-strain state of an infinite system. An obvious solution to this problem would be to update the EBCs periodically. This was difficult to perform in early simulations as the elastic field of the evolved system often became impossible to solve analytically. Recently, numerical techniques have been developed to solve the elastic field of the evolved atomistic system and to update the displacements of the boundary atoms (Ohsawa and Kuramoto, 1999). These techniques have naturally evolved into multiscale coupled models where atomistic and continuum approaches are interconnected (see Section 3). Still, even with continuously updated displacements of the boundary atoms, the dynamics of the system remain artificially constrained. Thus, EBC types of methods are commonly considered "static" methods.

An alternative to the EBC method is to apply external forces, instead of prescribed displacements, to the boundary atoms so that the stress at the boundary mimics the stress of an infinite system. The method is referred to as the "force (or traction) boundary condition" (FBC) method and was first introduced by DeCelis et al. (1983) to study fracture in iron and copper. The authors reported three major advantages of the FBC method versus the EBC method: (i) The FBC method allows for non-linear effects in the system as the boundary atoms remain unconstrained in their positions, while the EBC method uses linear elastic displacements, which lead to artifacts in the internal response; (ii) the thermodynamics of the system remains unaffected (for example, finite temperature simulations are readily achievable); and (iii) plastic deformation, caused for example by dislocation glide, is easily accommodated by the unconstrained boundaries in the FBC approach, while being restricted in the EBC approach.

As in the EBC approach, externally applied forces in the FBC approach also need to be periodically updated to follow the dynamics of the atomistic system. A drawback of the FBC method is the difficulty in precisely calculating the applied external forces at the atomic level to closely reproduce the atomic interactions of an infinite system. Reaction forces calculated by a continuum mechanics model are too approximate, and spurious effects, such as surface tension forces due to broken atomic bonds, appear and

make the system difficult to control and stabilize numerically. A method to eliminate surface tension was suggested by Cleri (Cleri, 2001) in the so-called "constant traction boundary conditions" molecular dynamics. This method of "constant traction boundary conditions" is currently used at NASA Langley Research Center (LaRC) to develop a novel multiscale coupling method based on the FBC approach and will be discussed in Section 3.2.8.

2.2.2 Overcoming Time Scale Limitations

The limitations on the length of system response time that can be simulated represent a serious obstacle in making useful predictions with atomistic MD simulations. To follow the atomic vibrations in an atomistic system, one has to integrate the atomic trajectories with a timestep of a few femtoseconds (10^{-15} s). Even with the current state-of-the-art gigahertz processors, the typical achievable simulation time is less than a nanosecond (10^{-9} s). Because the integration process is a sequential procedure, parallel computers cannot extend the simulation time, but can only make possible the simulation of larger systems for the same simulation time.

The very short timescale requires the application of unrealistically high strain rates for atomistic simulations (typically in the range of $10^{7} - 10^{12}$ s^{-1}). The high strain rates require high loads to be applied (of the order of gigapascals – 10^{9} Pa), which are often similar in magnitude to the theoretical shear strength of the material considered. In view of these unusually high numbers for both strain rate and magnitude of stress, it may seem surprising that MD simulations are successful in predicting and analyzing important physical processes and serving as a guiding tool for some experimental investigations. One of the main reasons for this success is the fact that the limitation of the short timescale is to a large extent compensated by the small length scale of these simulations. Small systems have much shorter response time, which means that the events take place much faster in an atomistic system than in an experiment. For example, a tensile uniaxial strain rate of 10^{7} s^{-1} applied to a 10 nm system would mean that the boundaries of the system will be moving apart at a speed of only 0.1 m/s.

The issue of the high strain rates in MD simulations was recently addressed in high-temperature deformation simulations of nanocrystalline Pd with grain sizes of approximately 10 nm (Yamakov et al., 2002). In spite of the extremely high strain rates ($> 10^7$ s^{-1}), these simulations quantitatively validated the Coble-creep equation (Coble, 1963) describing grain boundary diffusion creep in coarse-grained materials at strain rates of $< 10^{-4}$ s^{-1}. However, special care must be taken in low-temperature simulations to ensure that a process that might otherwise dominate the deformation behavior (that is, under experimental observation conditions) is not inadvertently suppressed, and hence overlooked, during the short time window to which MD simulations are inherently limited.

There are several methods, the so-called "accelerated dynamics methods" (recently reviewed by Voter et al., 2002), that are being developed to permit a substantial increase in the time window of MD simulations. In one of the methods, called the "hyperdynamics" method, the interatomic potential between atoms is carefully modified to decrease the activation barriers for so-called "infrequent events", such as vacancy migration governing lattice diffusion processes. Artificially decreasing the activation barriers dramatically increases the probability for occurrence of these "infrequent events", thus accelerating the evolution of the system by several orders of magnitude. In another method, called "temperature-accelerated dynamics", the temperature of the system is effectively increased while filtering out transitions that would not have occurred at the original temperature. This method also results in a dramatic increase in the dynamics of the system. In some systems, the overall acceleration may be as high as 10^7 orders of magnitude for various processes, thus extending the effective simulation time from nanoseconds to milliseconds.

A conceptually different approach is the "parallel replica method" (Voter, 1998) in which the original system is multiplied into many identical replicas and each one is evolved independently until an "infrequent event", such as an atomic jump between two lattice sides, takes place in one of the replicas. Then, the system that has undergone the

change is multiplied and its replicas overwrite the reminder of the systems. The process is repeated until the next "infrequent event" takes place in one or more of the replicas. This approach is considered to be the most accurate approach of all because it does not require any modifications of the interatomic potential or the temperature of the simulation, which may introduce unknown artifacts in the predicted system behavior. Additionally, it is well suited for use in parallel computing environments. The trade-off for the high accuracy is the relatively small effective time acceleration factor, which is equal to the number of replicas used (usually equal to the number of available processors in a parallel computation, typically of the order of 10^2-10^3). For additional time acceleration, the parallel replica method can be easily combined with the hyperdynamics method.

2.2.3 Interatomic Potentials

The interatomic potentials are used in atomistic simulations to define the force interactions between individual atoms in the simulated material. These potentials are analytic energy functions, which are simplified mathematical expressions that attempt to model the quantum mechanical interactions of electrons and nuclei. Their use is generally necessitated by the desire to model systems with sizes and time scales that exceed available computing resources required for quantum mechanics calculations. The goal of these potentials is to reproduce a variety of macroscopic physical properties of the simulated material, such as elastic constants, cohesive energy, melting temperature, vacancy formation energies, etc., by defining the elementary interactions between the atoms in a simple format suitable for fast computations.

In a recent review article, Brenner (Brenner, 2000) has identified four critical properties that an analytic potential energy function must possess in order to be effective:

1. *Flexibility:* A potential energy function must be sufficiently flexible to accommodate as wide a range of fitting data of material properties as possible;

2. *Accuracy:* A potential should be able to accurately reproduce the relevant material properties;
3. *Transferability:* A potential function should be able to describe at least qualitatively, if not with quantitative accuracy, structures not included in the fitting data base;
4. *Computational efficiency:* Evaluation of the potential should be relatively simple and computationally efficient, so that it can be computed many times over for all atomistic interactions and be fast enough to allow for the simulation of sufficiently large systems.

Satisfying all four criteria is a challenging task, and no general recipe exists for this purpose. While several standard potential functions have emerged for particular classes of materials, at present there is no definitive form that adequately describes all types of multi-atom bonding. Instead, potentials are often developed for specific applications with limited universality and transferability.

There are several functional forms of interatomic potentials. Early atomistic simulations employed pair centrosymmetric potentials, such as the Lennard-Jones (LJ) potential, which are functions only of the relative distance between two atoms. As it was recognized that centrosymmetric pair potentials cannot reproduce the elastic anisotropy of a material (e.g., the anisotropy factor $H = 2c_{44} + c_{12} - c_{11}$ is always zero; Johnson, 1972), efforts were directed to incorporate three-body interaction terms or many-body environmental dependent terms in the analytical expressions (Brenner, 2000).

Specifically for metals, the most successful form for a potential function is the "embedded-atom-method" (EAM) potential (Daw and Baskes, 1984), which is a combination of a centrosymmetric pairwise term, and a many-body term expressing a delocalized metallic bonding in the lattice. The EAM potential was found to accurately reproduce the properties of fcc metals, but it gave unsatisfactory results for bcc, hcp and transition metals. In addition, the surface energy was systematically underestimated for all systems. Later developments were able to significantly improve the surface energy

value by increasing the interaction range of the potential and including a larger number of interacting neighbors (Mishin et al., 1999).

However, non-fcc materials remained a challenge until a modified embedded atom method (MEAM) was suggested (Baskes, 1992) and applied to the study of silicon and germanium. The MEAM potential was successful in representing both metallic and covalent bonds, which made its use in simulations of heterogeneous multicomponent systems possible (e.g., hydrogen embrittlement of aluminum or iron). A drawback of the MEAM potential is its relatively high computational complexity, especially in calculating the derivatives that are needed to calculate the interatomic forces. A simpler and computationally more efficient form of the MEAM potential – angular dependent (ADP) EAM, which still preserves the original MEAM functionality, has been suggested recently by Mishin (Mishin, 2005). At present, EAM and MEAM potentials have been developed for most pure metals and a number of binary alloys.

3.0 Introduction to Multiscale Methods

Modeling atomistic processes quickly becomes computationally intractable as the system size increases. With current computer technology, the computational demands of modeling suitable domain sizes (on the order of hundreds of atoms for quantum mechanics-based methods, and potentially billions of atoms for classical mechanics-based methods) and integrating the governing equations of state over sufficiently long time intervals, quickly reaches an upper bound for practical analyses. In contrast, continuum mechanics methods such as the finite element method (FEM) provide an economical numerical representation of material behavior at length scales in which continuum assumptions apply. This strongly motivates the development of analytical multiscale methods to link macroscopic failure to the underlying atomic processes from which all material behavior originates.

Multiscale analysis is a class of systematic methodologies that have been developed to relate material behavior across length scales. Multiscale analyses attempt to

bridge length scales by providing different physics-based models that can appropriately represent damage mechanisms at each scale. In these approaches, models that best simulate the relevant physics at lower length scales are united with models at larger length scales through information transfer involving averaging, homogenization, or superposition schemes. The ultimate success of this approach is dependent on the accuracy of data linkage and the intrinsic fidelity of the physical models used.

3.1 Classification of Multiscale Approaches

Multiscale methods may be generally classified as either concurrent or sequential (Liu et al., 2004; Park et al., 2004). These methods are becoming valuable tools for linking micro- and macroscopic material behavior to atomic level processes.

Concurrent multiscale analysis involves solving two or more strongly linked material models simultaneously. A general schematic of concurrently coupled atomic and continuum regions is depicted in Figure 3. In general, there exists a domain representing material at the atomic level (e.g. MD) and a domain representing material at a continuum level (e.g. FEM). An intermediate region involves an interface between

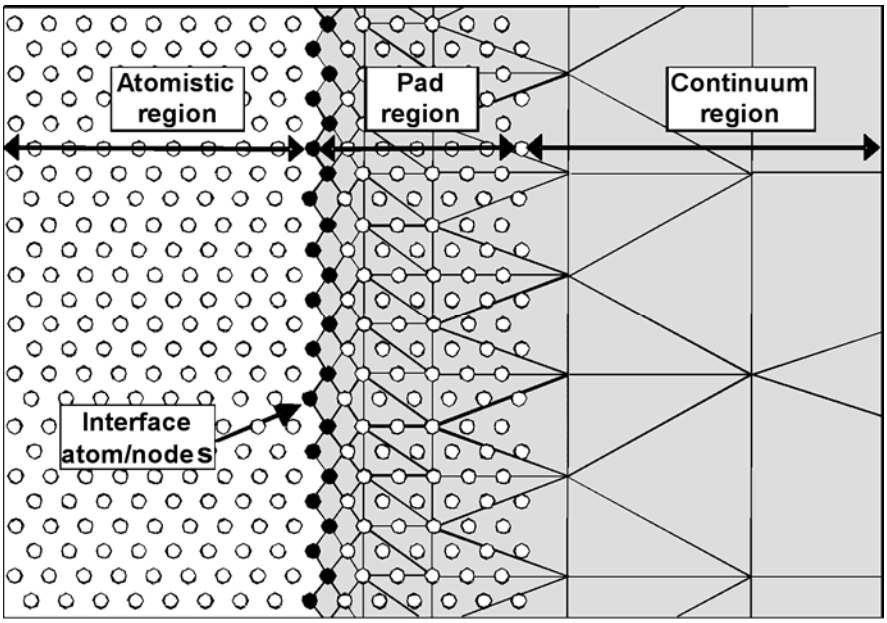

Figure 3. General schematic of coupled atomistic/continuum regions.

these two different computational procedures that typically includes an overlap region of "pad" atoms/nodes in which different coupling schemes are used.

Some approaches, however, can consist of a combination of both sequential and concurrent schemes, and others, such as a recently developed procedure based on multiscale boundary conditions, can fall far enough outside these two designations to constitute an independent approach (Park and Liu, 2004). Many multiscale modeling strategies have been explored in recent years, and the most well established state-of-the-art methods will be discussed.

Sequential modeling typically involves some form of averaging of physical parameters that can serve as initial conditions or provide material parameters to another model which is analyzed separately. A desirable aspect of sequential methods is that length and time scales between independent material models do not have to be coupled. The averaging or homogenization of information across length scales that is inherent to sequential multiscale methods is depicted in Figure 4 where a notional coupling is shown across domains representing characteristic features at the sub-atomic through structural scales.

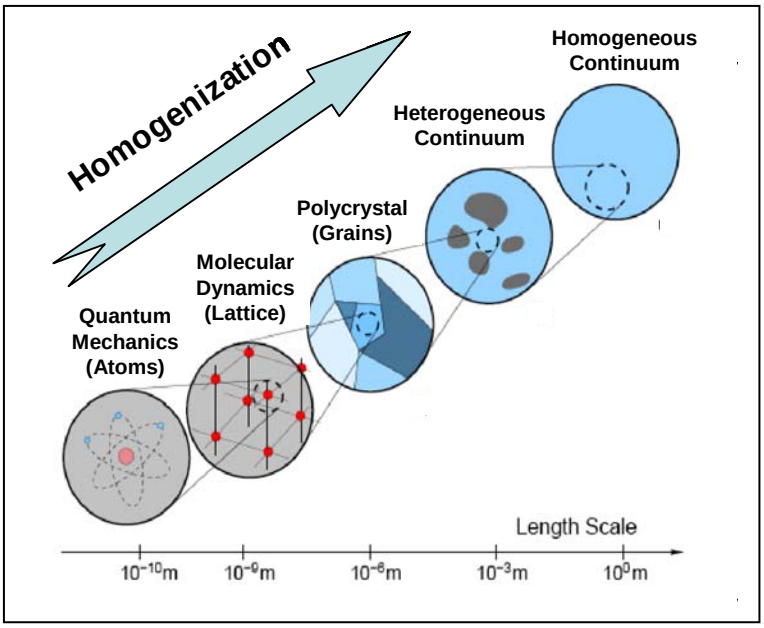

Figure 4. Hierarchy of models over length scales.
(Adapted from Oden et al., 2006)

3.2 Concurrent Multiscale Methods

Concurrent methods are being continuously developed and enhanced by the materials science community. The common approach of the concurrent methods is to identify a small region of the simulated system where the representation of material is performed at the atomic level. This atomistic region is embedded into a larger surrounding region where the material is represented at the continuum level. In developing analytical approaches using this simulation paradigm, a primary concern has been the seamless coupling of forces and displacements between the different models at the interface between the two regions. The inherent mismatch between computational frameworks – atomistic (such as molecular-dynamics or molecular-statics) and continuum (such as finite element or finite difference) methods – and the differing representation of material properties can lead to simulation difficulties.

In order to achieve a successful coupling, the usual approach is to refine the continuum representation (the FE mesh or the finite difference grid) down to the atomic scale by superposing each node to an atom at the interface region (Figure 4). In this way, the atomistic degrees of freedom – position and momentum of each atom – are identified directly with the continuum degrees of freedom – nodal displacements and their derivatives. Several extensive reviews of concurrent methods have been presented in the literature (Liu et al., 2004; Park and Liu, 2004; Oden et al., 2006). While numerous variations on basic procedures for coupling atomistic and continuum domains exist, only a handful have been well-developed and have gained a measure of widespread use. A brief review of these methods, representing the current state-of-the-art, follows.

3.2.1 The Macroscopic, Atomistic, Ab initio Dynamics Method

The MAAD (Macroscopic, Atomistic, Ab initio Dynamics) procedure was developed to simulate fracture by combining ab initio quantum analysis, molecular dynamics, and finite element continuum models (Broughton et al., 1999; Abraham et al., 2000; Shen, 2004a). The ab initio analysis utilizes tight binding (TB) procedures to

predict bond breakage at the crack tip, molecular dynamics (MD) based on empirical force potentials to model the crack wake and surrounding atomic lattice, and a finite element (FE) model to simulate the far-field material. A total Hamiltonian describes the dynamics of the system by combining Hamiltonians of the three separate regions and their interfaces. In this approach, the FEM nodes correspond in a one-to-one manner with the interface atoms of the MD region. Figure 5 shows the basic division of the overall simulation into regions governed by different computational methods.

Two significant issues have been raised regarding the MAAD approach. One is that the timestep used to integrate the governing equations in each of the three domains is equal to the smallest step required in any of them, causing a large increase in computational cost. Another issue is the lack of damping, which may be needed to remove spurious reflections at the interfaces between the three regions.

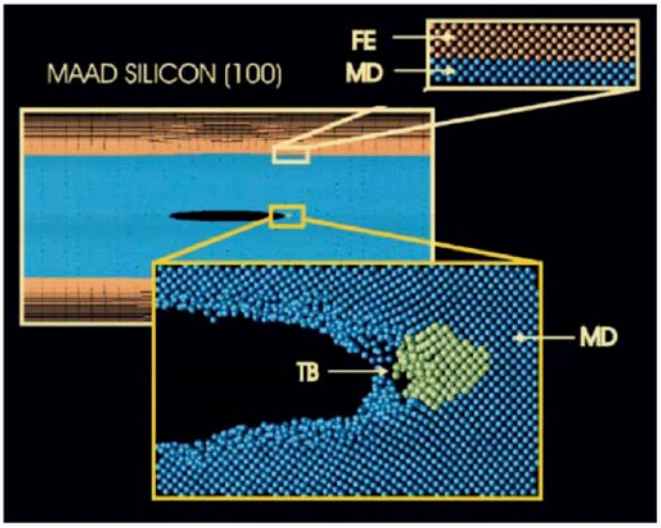

Figure 5. Structure of MAAD coupling. (From Buehler, 2006)

3.2.2 The Finite Element-Atomistic Method

The FEAt (Finite Element-Atomistic) method (Kohlhoff, et al., 1991; Gumbsch and Beltz, 1995; Gumbsch, 1995) is a methodology similar to MAAD that links atomistic

representation to a continuum finite element field. Both FEAt and MAAD utilize a domain of "pad" atoms in the overlapping region of the MD-FEM interface in which individual atoms are directly linked to finite element nodes. These regions are shown in Figure 6. An interesting feature of FEAt is that non-local elasticity theory (Kroner, 1967) is used in the pad region to describe the continuum representing the finite range of atomistic forces and can be considered as a continuation of the lattice. These approaches have been successfully applied to the problem of crack propagation.

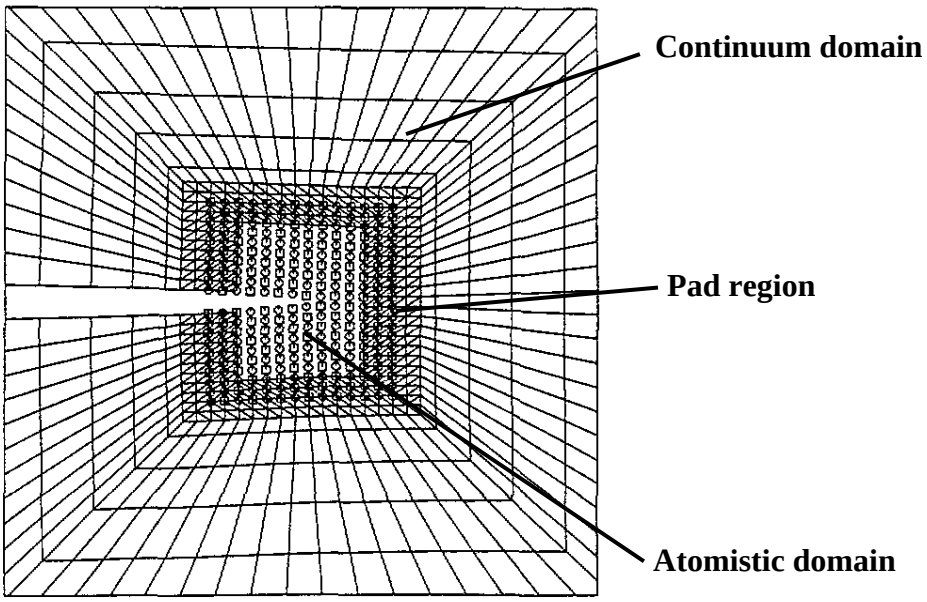

Figure 6. FEAt model of a crack tip in an fcc crystal.
(From Gumbsh and Beltz, 1995)

3.2.3 The Coarse Grained Molecular Dynamics Method

A generalized formulation of the conventional FEM utilizes FEM nodes superposed over the entire material domain to develop another computational scheme for atomistic-continuum coupling called Coarse Grained Molecular Dynamics (CGMD) (Rudd and Broughton, 1998, 2005). In this approach, a MD region is defined in which refinement is made such that a one-to-one atom-node linkage exists. Outside this region,

the finite element mesh is coarsened with individual nodes associated with many atoms. It is this coarse-grained (CG) finite element region that reduces the computational cost of representing the entire material domain. Thus, the MD region is solved using the integrated equations of motion for each atom, while the kinematics of the nodal degrees of freedom in the CG region are obtained using the equations of continuum FEM. A benefit of the CGMD method is that the interface between the MD and CG regions reduces spurious elastic wave scattering compared to other MD-FEM coupling methods. The MD and finite element CG regions are shown in Figure 7.

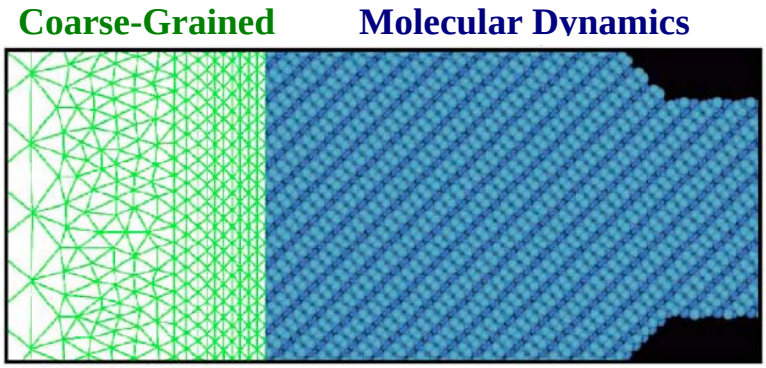

Figure 7. Depiction of CG and MD regions in the CGMD approach. (From Rudd and Broughton, 2005)

3.2.4 The Quasicontinuum Method

The Quasicontinuum (QC) method was originally formulated to provide a direct coupling of an atomistic region to a continuum domain (Tadmor et al., 1996; Miller et al., 1998; Knap and Ortiz, 2001; Miller and Tadmor, 2002). The QC method is based on an atomic description of the material domain and uses deformation gradients and the Cauchy-Born rule (Born and Huang, 1954) for homogeneous deformations to assign "representative atoms" or "repatoms" to describe individual atoms or enforce kinematic constraints on clusters of atoms that are considered as a local continuum. The basic assignment of atoms and possible partitioning of the QC region into local continuum domains and MD domains is shown in Figure 8. Continuum regions utilize FEM shape

functions over the domain, and material properties are obtained by a summation of the empirical potential function of the atoms contained in these regions. Remeshing is intermittently performed to update the model to resolve atomic scale detail where needed and to reform continuum atomic subdomains where deformation gradients are small to minimize computational cost. The method is commonly applied to 2-D problems and, because of the direct one-to-one relation between repatoms, was originally restricted to zero Kelvin temperature states.

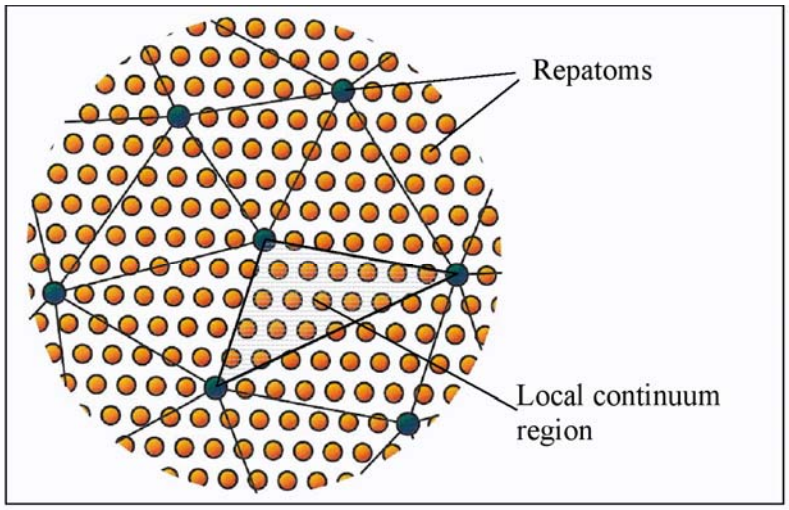

Figure 8. Repatoms used to define individual atoms and local continuum regions in the QC method. (From Knap and Ortiz, 2001)

A finite temperature QC method has subsequently been developed (Shenoy et al., 1999; Miller and Tadmor, 2002). The method offers a direct transition between atomistic and continuum fields and can effectively follow the evolution of atomistic mechanisms such as dislocation nucleation and crack propagation. However, special treatments are required to remove spurious "ghost forces" at the interface, to mitigate free-surface effects, and to account for finite temperature states. The QC method offers a general modeling technique and has been applied to simulate nanoindentation, fracture, dislocation motion, and interaction of grain boundaries.

3.2.5 The Bridging Domain Method

Another representative concurrent coupling approach is the bridging domain method (Belytschko and Xiao, 2003; Xiao and Belytschko, 2004) and is based on an overlay approach in which MD and FEM representations are superposed in an interface region. This method relaxes the strict atom-node correspondence required in many other methods by allowing interpolation of FEM nodal displacements to be associated with atomic displacements in the bridging domain. The bridging domain with atom-finite element node overlap is shown in Figure 9. The method explicitly develops coupled energy Hamiltonians for the atomistic and continuum regions and enforces compatibility in the bridging domain using Lagrange multipliers. Dynamic behavior is simulated through an explicit algorithm that includes a multiple time-step scheme. This approach also avoids spurious wave reflection at the MD/FEM interface without introducing damping or filtering procedures.

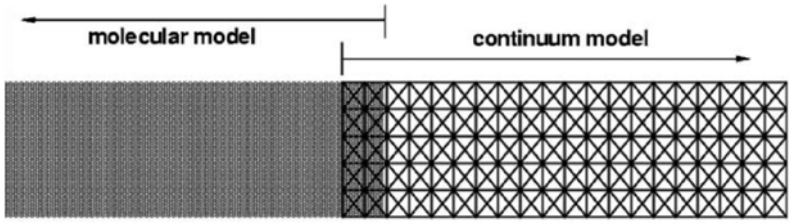

Figure 9. Application of bridging domain coupling method in 2-D. (From Xiao and Belytschko, 2004)

3.2.6 The Coupled Atomistic/Discrete Dislocation Method

The CADD (Coupled Atomistic/Discrete Dislocation) method (Shiari et al., 2005; Shilkrot et al., 2002a, 2002b; Curtin and Miller, 2003; Shilkrot et al., 2004) is specifically designed for problems in which dislocation formation and interaction are the physical mechanisms of interest and persist over long distances. The coupling at the interface is similar to the MAAD and FEAt methods in that it uses a pad region in which "handshaking" between atomic and continuum degrees of freedom occurs. CADD is formulated to identify the type of dislocation approaching the MD/FEM interface from

the atomic domain and then pass the dislocation into a surrounding discrete dislocation domain. Passing the dislocation is accomplished through an ad hoc addition and subtraction procedure. The operation involves adding analytical equations describing the displacement and stress fields of the dislocation to the continuum discrete dislocation domain and adding the forces associated with a negative image of the dislocation into the atomistic domain to realign the stacking fault, thus eliminating the original dislocation. The passed dislocations continue to interact with the MD domain through displacement boundary conditions at the interface. A detection band is created near the MD-FEM interface to determine the type of dislocation entering the continuum (eg., an edge or screw dislocation). This detection scheme is shown in Figure 10 where, for 2-D dislocations, active slip planes of a face centered cubic (fcc) metal are separated by relative angles of $\pi/3$.

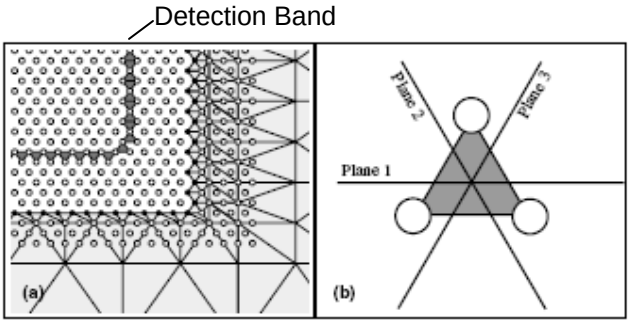

Figure 10. Close-up of dislocation detection band near interface. (From Shilkrot et al., 2004)

The continuum is assumed linear elastic such that a superposition can be made to decompose the continuum into an infinite domain that contains the long-range singular dislocation stress fields modeled using dislocation dynamics and a finite domain region that contains smooth displacement fields modeled using FEM. The decomposition of the coupled MD-FEM domain in CAAD is shown in Figure 11 with (I) depicting the infinite discrete dislocation region, (II) showing the bounded region defined by finite elements, and (III) illustrating the purely atomistic region. The infinite discrete dislocation region represents dislocations as superposed analytic solutions. In the figure, Ω and $\partial\Omega$ represent volumes and surface regions, respectively, and *T*, *f*, and *u* represent tractions, forces and displacements, respectively. The subscripts *0*, *C*, *A*, and *I* designate the

original combined system, the continuum region, the atomistic domain, and the interface, respectively and the '~' and '^' overbars represent the discrete dislocation field and the finite element field, respectively.

This method directly addresses the representation of discrete dislocation (DD) plasticity in a continuum field using established DD methods (van der Geissen and Needleman, 1995). Because the dislocations are represented analytically, a computationally demanding full atomic simulation is not required, yielding a significant improvement in modeling efficiency. The transition between the atomic and continuum finite element domains utilizes a one-to-one node-atom linking that directly ties the interface atoms to the nodes in the continuum. An extension of the atomic region into the continuum is assumed in which pad atoms are superposed with continuum elements and are connected to nodal displacements (see Figure 3). These atoms minimize the effect of the free surface on the interface atoms but contribute a modeling error by introducing nonphysical stiffness along the interface. CADD is currently restricted to simulating dislocations in two dimensions.

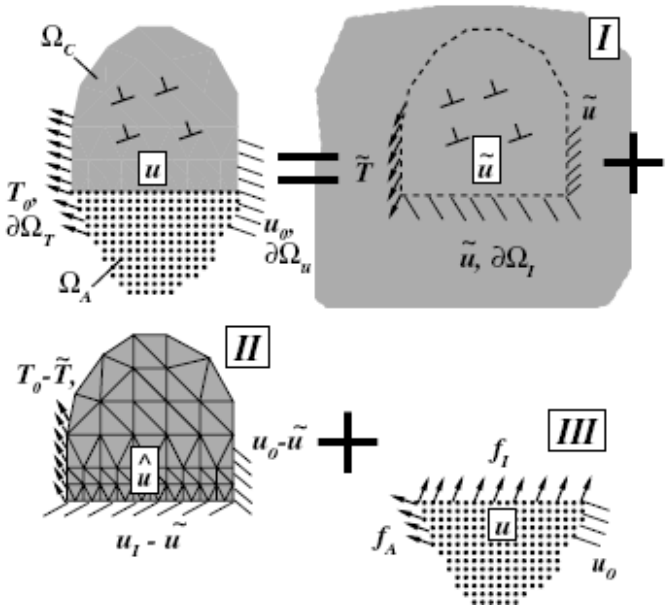

Figure 11. Decomposition of coupled MD-FEM domain using linear superposition. (From Shilkrot et al., 2004)

3.2.7 The Equivalent Continuum Model

A combined MD and Equivalent Continuum Model (ECM) method has been developed (Shen and Atluri, 2004b), which is similar to the Quasi-continuum methods, but uses the meshless local Petrov-Galerkin (MLPG) representation to link the MD and ECM regions. In general, meshless methods are developed to overcome some of the disadvantages of the finite element method, such as the need to interpolate discontinuous secondary variables across interelement boundaries and the need for remeshing in large deformation problems. The Cauchy-Born hypothesis is applied in the ECM region for determining the elastic properties of the continuum from the atomistic description of the system. The ECM and MD regions are depicted in Figure 12.

As shown in Figure 12, in the MD region, the solid points represent atoms, while in the ECM region, the solid points represent atoms and the open points represent nodes used in the MLPG method. Thus, in the ECM region, atoms and nodes do not have to be coincident. The ECM method has been demonstrated in one-dimensional chain models and in the two-dimensional analysis of a one-atom thick planar graphite sheet.

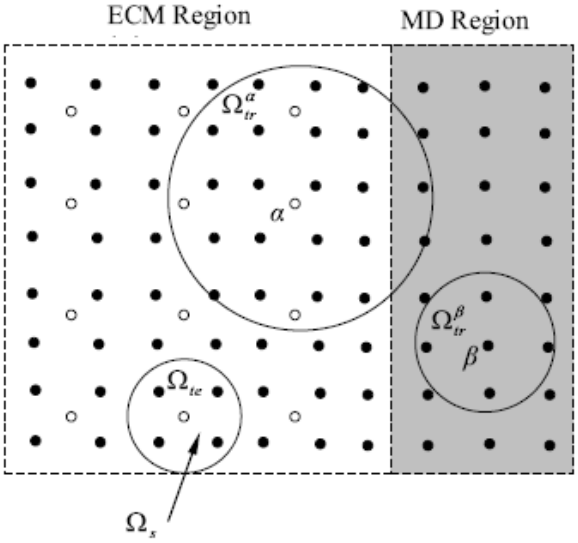

Figure 12. Depiction of ECM and MD region in the MLPG approach to MD-FEM coupling. (From Shen and Atluri, 2004b)

3.2.8 The Embedded Statistical Coupling Method

A recently developed approach to MD-FEM coupling has been developed based on a restatement of the typical boundary value problem used to define a coupled domain (Saether et al., 2007 and Saether, et al., 2008). The method uses statistical averaging of the atomistic MD domain to provide displacement interface boundary conditions to the surrounding continuum FEM region, which, in return, generates interface reaction forces applied as piecewise constant traction boundary conditions to the MD domain. The coupled MD-FEM regions are depicted in Figure 13. The two systems are computationally disconnected and communicate only through a continuous update of their boundary conditions. With the use of statistical averages of the atomistic quantities to couple the two computational schemes, the developed approach is referred to as an embedded statistical coupling method (ESCM) as opposed to a direct coupling method where interface atoms and FEM nodes are individually related. The structure of the ESCM approach is depicted in Figure 14 where the MD region near the FEM interface is partitioned into a series of Interface Volume Cells (IVCs) and Surface Volume Cells (SVCs) that are used to interface with the surrounding FEM nodes. The methodology is inherently applicable to three-dimensional domains, avoids discretization of the continuum model down to atomic scales, and permits arbitrary temperatures to be applied.

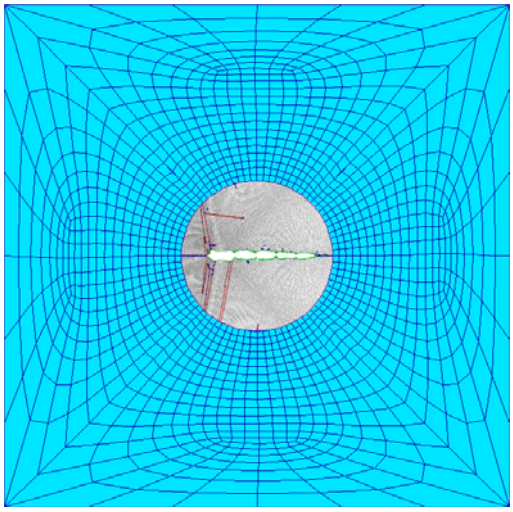

Figure 13. An embedded MD region within an FEM domain. (Saether et al., 2007)

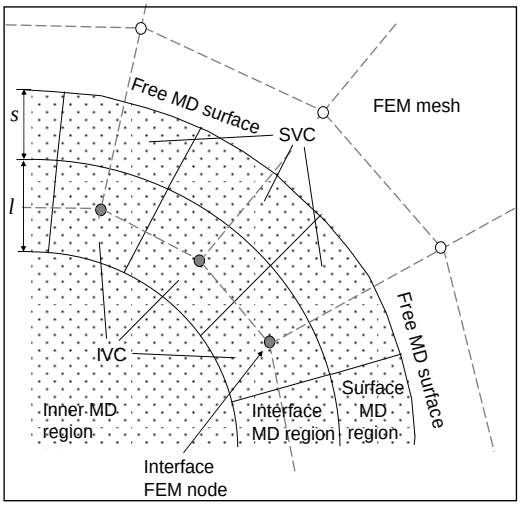

Figure 14. Structure of the ESCM. (Saether et al., 2007)

3.2.9 Issues in the Development of Concurrent Methods

Various modeling issues often arise that need to be addressed to formulate successful concurrent coupling methodologies. These issues naturally arise in the attempt to join computational domains that are modeled by distinctly different representational frameworks of the operant physics, namely, atomistic (MD) and continuum mechanics (FEM) methods.

In MD, atoms are influenced by the nonlocal force interactions of neighboring atoms, while in typical FEM methods, all quantities are local to a material point. With the nonlocal interaction in the MD region and the local interaction in the continuum, linking the two can cause a loss of force reciprocity at the interface and a violation of momentum conservation due to induced "ghost" forces. From a theoretical standpoint of establishing the governing equilibrium equations, it has been observed (Curtin, 2007) that most concurrent coupling methods that obtain equilibrium from the variation of an energy functional lead to some sort of spurious force generation at the interface, while those methods based on summing forces to zero at the interface tend to avoid these spurious effects.

Also, inelastic material processes, such as dislocations in the MD region, must be transformed into continuum plasticity in the FEM domain. This transformation is difficult to theorize and remains an open issue. Additionally, a common difficulty involves material mismatch as higher-order material constitutive behavior included in the energy potentials for atomic interactions is problematic to simulate in the constitutive relations used in the FEM.

Finally, the MD-FEM interface typically generates spurious reflections of phonons that must be damped out. One possible solution involves implementation of a dynamic continuum to allow phonons to be transferred from the MD to the continuum region; however, the use of a dynamic continuum requires much smaller time steps than a quasi-static continuum, thereby incurring a large computational cost. Even with a

dynamic continuum, a coarse FEM mesh in the region far from the interface acts as a filter that naturally reflects stress waves of increasing wavelengths back to the MD region.

3.3 Sequential Multiscale Methods

Sequential – or "hierarchical" - methods are typically used for modelling heterogeneous materials for which different constitutive laws are required at different length scales. The total material deformation and stress and strain fields are typically decomposed into the sum of a coarse macro-component and a fine micro-component. The fine and coarse fields are determined through separate analyses and are summed to obtain the solution for the total field (Oden et al., 1999; Tadmor, et al., 2000; Clayton and Chung, 2006; Wagner and Liu, 2001; Hao et al., 2004).

A notional flow of sequential coupling that utilizes cohesive zone models (CZMs) to carry information of microscopic failure mechanisms to predict damage progression at larger length scales is depicted in Figure 15 (from Glaessgen et al., 2005) . In Figure 15, CZMs provide the critical transition between inherently atomistic and inherently continuum representations. In the figure, δ_i represent individual displacements while λ_i represent relative displacements across a surface, i.e. $\lambda_i = \delta_i^{top} - \delta_i^{bot}$. Elsewhere, the notation Δ_i is used to represent combinations of relative displacements in mixed-mode applications such that $\Delta_i = f(\lambda_I, \lambda_{II}, \lambda_{III})$. These quantities are often used interchangeably in the literature. Because of their importance and pervasive use in sequential multiscale analysis, the present discussion will focus on CZM-based methods.

3.3.1 Cohesive Zone Models

Cohesive zone models were originally developed to represent complicated nonlinear fracture processes in ductile and quasi-brittle materials (Dugdale, 1960; Barenblatt, 1962). CZMs were later developed to describe general adhesion and frictional slip along an interface (Maugis, 1992; Kem et al., 1998). The CZM approach

is formulated on a constitutive relationship based on applied tractions and relative displacements to represent separation in various fracture modes of two initially coincident surfaces. The relative displacements associated with the creation of a new fracture surface for the three fundamental fracture modes are depicted in Figure 16.

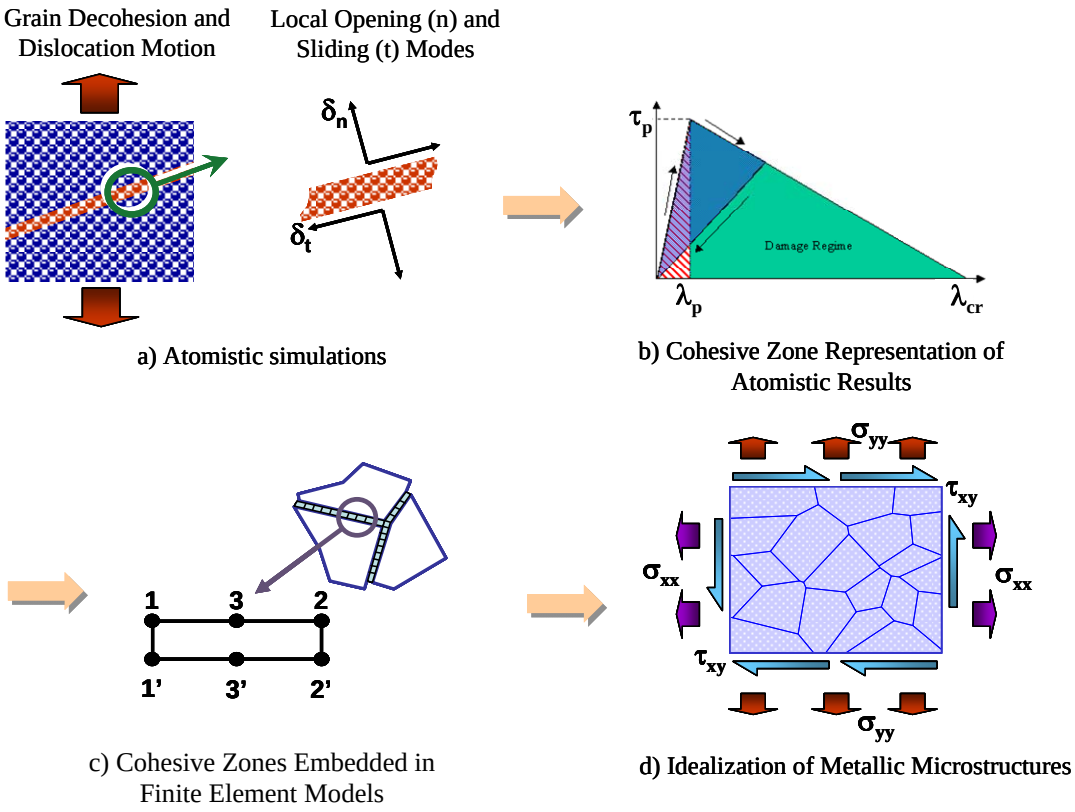

Figure 15. Multiscale analysis with cohesive zone models.

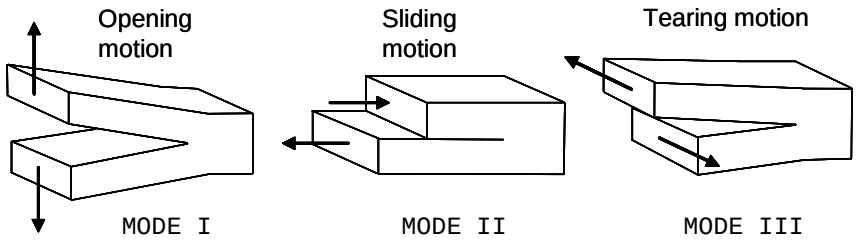

Figure 16. Fundamental fracture modes in solids

In the CZM approach, the area under the CZM traction-displacement curve represents the work of separation to grow a crack in a particular fracture mode, i.e. the fracture toughness, and is given by Tvergaard and Hutchinson (1992) as

$$G_c = \int_0^{\Delta^f} \tau d\Delta \tag{2}$$

where G_c is the work of separation, τ is the applied traction, Δ is a general form of the displacement, and Δ^f is the critical displacement at which complete separation has occurred and the tractions are zero.

In general, the traction-displacement relationships $\tau(\Delta)$ are obtained by differentiation of a potential $\phi=\phi(\Delta)$, which represents the free energy of decohesion. The selection of a potential function is typically based on recovering the assumed traction-displacement relationship, and particular forms are generally selected for analytical convenience. In practice, various forms have been used as shown in Table 1. The existence of a work potential yields the work of separation regardless of the shape of the function.

CZMs have been developed using different work potentials and different mathematical forms, and applied to different material systems at different length scales. Because of the wide range of variability in CZM formulations and applications, a broad survey of representative work will be presented here.

Cohesive properties along an interface have typically been approximated using empirical data to define the CZMs (Tvergaard and Hutchinson, 1992; Costanzo and Allen, 1995; Camacho and Ortiz, 1996; Klein and Gao, 1998; Zavattieri et al., 2001; Zavattieri and Espinosa, 2003; Turon et al., 2004). These models are frequently used in conjunction with the finite element method (FEM) to study fracture at macroscopic length scales in a wide variety of materials.

Wei and Anand (2004) have used a modified CZM model to study intergranular fracture in nanocrystalline Ni. In their FEM simulation, the CZM-based decohesion element approximated both reversible and irreversible inelastic sliding-separation deformations at the grain boundaries prior to failure. The parameterization of the model was performed by using available experimental data for stress-strain curves of nanocrystalline Ni with a large number of grains. Iesulauro (2002) has also applied the CZM technique to simulate fatigue crack initiation in Al polycrystals in which a statistical representation of bulk material properties was input to the CZM.

The shape of the CZM law represents the basic macro-scale behavior of the material near the crack (tip) under load. Various attempts have been made to determine the shape based on fundamental bonding characteristics in metals (Rose et al., 1983; Nguyen and Ortiz, 2002). The most commonly assumed forms of the traction-displacement law have been expressed as exponential, bilinear, and trapezoidal functions. A general review of various forms of CZMs is found in Chandra et al. (2002). Table 1 shows a range of various CZM functions that have been presented in the literature and embedded into CZM elements. The table illustrates the basic form of the CZMs, their key parameters, and important features.

Despite all of the forms of CZMs that have been proposed, a common mathematical form not shown in Table 1 is a bilinear constitutive relation. The bilinear form is often chosen because of its mathematical simplicity and because of its suitability for representing brittle and ductile fracture in metals (Yamakov, et al., 2006) and brittle fracture in polymeric and ceramic composite materials (Camacho and Ortiz, 1996). This form of CZM is shown in Figure 17.

Bilinear types of cohesive zone models were used in several recent FE simulations of brittle fracture during multi-axial dynamic loading of ceramic microstructures (Zavattieri et al., 2001, 2003).

Table 1. Various cohesive zone models and their parameters. (From Chandra et al., 2002)

Author (year)	Proposed model	Model parameters	Problem solved	Model constants	Comments
Barenblatt (1959, 1962)	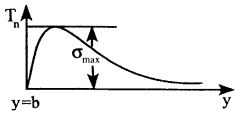	$K = \int_0^{d+d'} \frac{G_1(t)\,dt}{\sqrt{t}}$ $= \sqrt{\frac{\pi E T_0}{1-\nu^2}}$ (ductile) $= \sqrt{\frac{\pi E T_0}{1-\nu^2}}$ (brittle) $T = T_0 + T_1$ T_0 is work of separation for brittle materials T_1 is work of plastic deformation	Perfectly brittle materials		The first to propose the cohesive zone concept
Dugdale (1960)	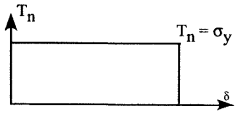	$\frac{s}{a} = 2\sin^2\left(\frac{\pi}{4}\frac{T}{\sigma_y}\right)$ For small value of T/σ_y $\frac{s}{l} = 1.23\left(\frac{T}{\sigma_y}\right)^2$	Yielding of thin ideal elastic–plastic steel sheets containing slits	Plastic zone ranges from 0.042 to 0.448 (in.)	Cohesive stress equated to yield stress of material
Needleman (1987)	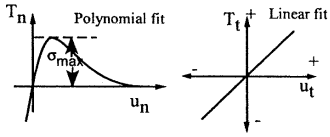	ϕ_{sep} is work of separation δ are normalizing parameters σ_{max} is cohesive strength	Particle-matrix decohesion	$\delta = 10^{-9}$ to 10^{-8} m cohesive energy 1–10 J/m^2 $\sigma_{max} = 1000$–1400 MPa $\sigma_y = 350$–450 MPa	Phenomenological model; predicts normal separation
Rice and Wang (1989)	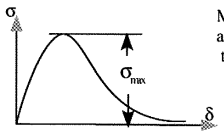 Model based on atomic fit of the type $(1+x)e^{-x}$	E_0 is initial Young's modulus h is normalizing parameter σ_{max} is maximum stress α is constant $\left(\frac{E_0 h}{\alpha^2} = 2\gamma\right)$	Solute segregation		Ascending part is equated to E_0 considers normal separation and ignores shear separation
Needleman (1990a)	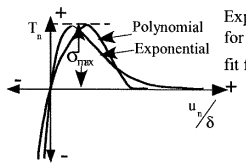 Exponential fit for T_n. Linear fit for T_t	ϕ_{sep} is work of separation δ are normalizing parameters σ_{max} is cohesive strength	Particle-matrix decohesion	$\delta = 10^{-9}$ to 10^{-8} m	Predicts normal separation
Needleman (1990b)	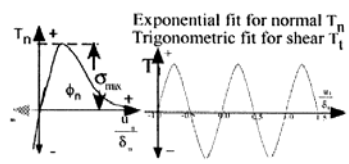	ϕ_n, ϕ_t are work of normal and shear separation δ_n, δ_t are critical displacements σ_{max} is cohesive strength	Decohesion of interface under hydrostatic tension	$\delta_n = \delta_t = 2 \times 10^{-10}$ to 2×10^{-9} m $J_{tc}/\phi_n = 0.57$–2.59 $\sigma_{max}/\sigma_0 = 2, 3$	Periodic shear traction to model Pieriels shear stress due to slip
Tvergaard (1990)	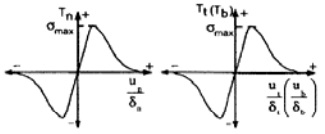	δ_n, δ_t are critical displacements σ_{max} is cohesive strength	Interfaces of whisker reinforced metal matrix composites	$\delta_n = \delta_t = 1 \times 10^{-9}$ m $E = 60$ GPa (Young's mod) $\sigma_y/E = 0.005$ $\sigma_{max}/\sigma_y = 5$–9	Quadratic model
Tvergaard and Hutchinson (1992)	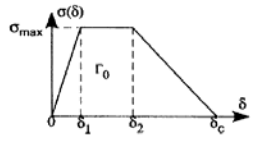	Γ_0 is work of separation δ_c is critical displacement σ_{max} is peak normal traction /interface strength δ_1, δ_2 are factors governing shape	Crack growth in elasto-plastic material, peeling of adhesive joints	$\Gamma_{ss}/\Gamma_0 = 0$–10 (Γ_{ss} = Pl wk.), $\delta_n^c/\delta_t^c = 1$ $\sigma_{max}/\sigma_y = 0$–14 δ_1, $\delta_2 = 0.15, 0.5$ $\sigma_y/E = 1/300$	Claims shape of separation law are relatively unimportant
Xu and Needleman (1993)	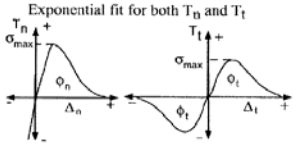	ϕ_n is work of normal separation ϕ_t is work of shear separation δ_n, δ_t are critical displacements σ_{max} is cohesive strength	Particle-matrix decohesion	$\delta_n = \delta_t = 2 \times 10^{-10}$ to 2×10^{-9} m	Predicts shear and normal separation

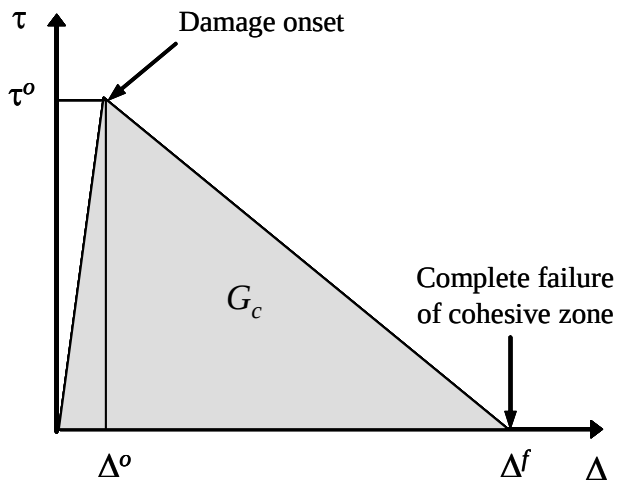

Figure 16. Bilinear cohesive zone model.

3.3.1.1 Mixed-Mode Representation using CZMs

Specific examples of mixed-mode applications of CZMs have been presented in the literature and are discussed here. Among these applications, Ortiz and Pandolfi (1999) developed a CZM approach for simulating 3-D crack propagation and considered displacement jumps associated with normal opening, δ_n, and shear opening, δ_s. They accounted for mode coupling by a simple device of introducing an effective opening displacement given by

$$\delta = \sqrt{\beta\delta_s^2 + \delta_n^2} \tag{3}$$

where the parameter β assigns different weights to the sliding and normal opening displacements. A simple model of cohesion is then obtained by assuming that the free energy potential, ϕ, depends on δ through the effective opening displacement, i.e.,

$$\phi = \phi(\delta, q) \tag{4}$$

where q is a collection of internal state variables that describe inelastic processes that coexist with decohesion. A potential of the form

$$\phi = e\sigma_c\delta_c\left[1-\left(1+\frac{\delta}{\delta_c}\right)e^{-\delta/\delta_c}\right] \tag{5}$$

is developed where $e \approx$ 2.71828, σ_c is the maximum normal traction, and δ_c is a characteristic opening displacement. Irreversibility is incorporated into the cohesive laws in the sense that the cohesive surfaces are assumed to unload linearly to the origin. The resulting exponential traction-displacement curve is shown in Figure 18(a-b). Similarly, a bilinear traction-displacement curve with a similar peak traction is shown in Figure 18(c-d).

A 3-D CZM accounting for Mode I opening, Mode II sliding, and Mode III tearing has been developed (Segurado and LLorca, 2004) to study decohesion in composite materials consisting of elastic spheres within an elasto-plastic matrix. The assumed form of the cohesive zone for normal opening is depicted in Figure 19. An exponential CZM is used to represent Mode I fracture while a linear relation is used for simulating tangential fracture modes. Unloading after softening is assumed to follow a path directly back to the origin.

As mentioned previously, tractions are typically derived from a single elastic potential. In this case, the potential is given by

$$\begin{aligned}\phi(\Delta u_n, \Delta u_{t1}, \Delta u_{t2}) = \frac{27 t_c \Delta u_c}{4}\Bigg\{&\frac{1}{2}\left(\frac{\Delta u_n}{\Delta u_c}\right)^2\left[1-\frac{4}{3}\frac{\Delta u_n}{\Delta u_c}+\frac{1}{2}\left(\frac{\Delta u_n}{\Delta u_c}\right)^2\right]\\ &+\frac{\gamma}{2}\left(\frac{\Delta u_{t1}}{\Delta u_{t2}}\right)^2\left[1-2\frac{\Delta u_n}{\Delta u_c}+\left(\frac{\Delta u_n}{\Delta u_c}\right)^2\right]\\ &+\frac{\gamma}{2}\left(\frac{\Delta u_{t2}}{\Delta u_c}\right)^2\left[1-2\frac{\Delta u_n}{\Delta u_c}+\left(\frac{\Delta u_n}{\Delta u_c}\right)^2\right]\Bigg\}\end{aligned} \tag{6}$$

for $\Delta u_n < \Delta u_c$, where Δu_n is the normal relative displacement, and Δu_{t1} and Δu_{t2} are the tangential relative displacements between the crack surfaces. The term t_c is the maximum normal stress carried by the interface undergoing purely normal separation, and Δu_c is the relative normal displacement at which all the cohesive forces vanish. The parameter γ specifies the ratio of normal to shear stiffness of the interface, where $\gamma = 0$ indicates that the cohesive element only transfers normal stresses. The normal and tangential tractions at the interface can be computed by taking the partial derivatives of the potential with respect to the corresponding relative displacements. Other examples of similar mixed-mode CZM formulations can be found in Li and Chandra (2003), Chandra and Shet (2004), Li and Siegmund (2004)

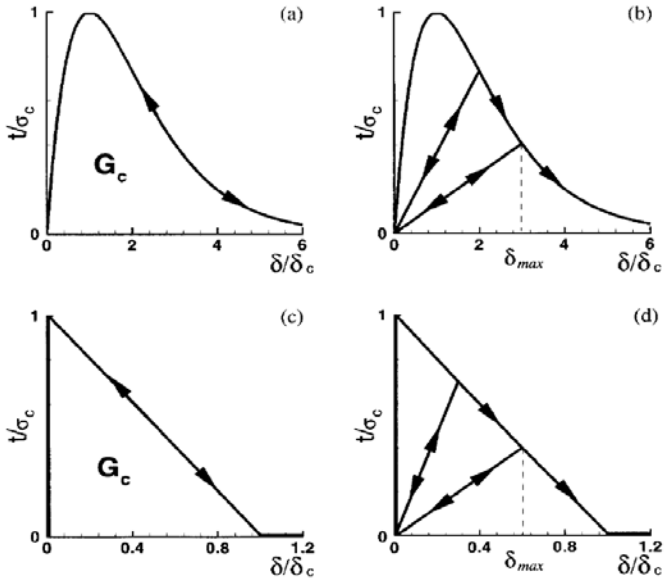

Figure 18. Two assumed CZM curves. (a) Exponential traction-displacement law with (b) loading-unloading rule. (c) Bilinear traction-displacement law with (d) loading-unloading rule. (From Ortiz and Pandolfi, 1999)

Mixed-mode CZM models have also been determined through direct interpolation between individual single-mode CZMs (Turon et al., 2004). In this approach, a traction-displacement law is assumed in which normal and shear components of the traction and displacement are interpolated based on mode mixity. The interpolated or effective CZM

relates a combined traction to a combined displacement jump. The effective CZM is used to determine a state variable that describes the damage state used to modify the stiffness of the cohesive zone. An outline of the basic formulation follows.

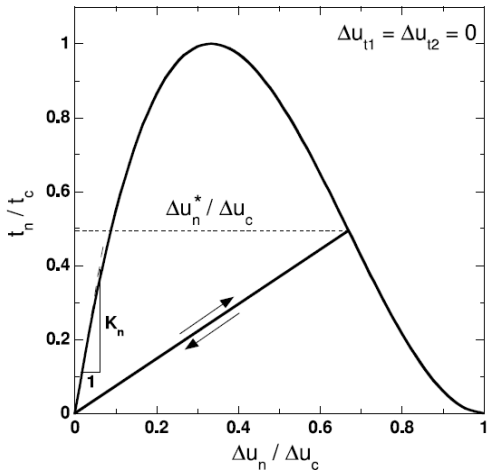

Figure 19. Normalized opening traction-displacement relation. (From Segurado and LLorca, 2004)

The interpolation of CZM components is depicted in Figure 20. Relative displacement jumps between the upper and lower nodes, $\Delta = \Delta^{top} - \Delta^{bot}$, corresponding to the maximum traction, indicate the onset of damage. Final failure of the cohesive zone is assumed after the relative displacement jump yields zero traction.

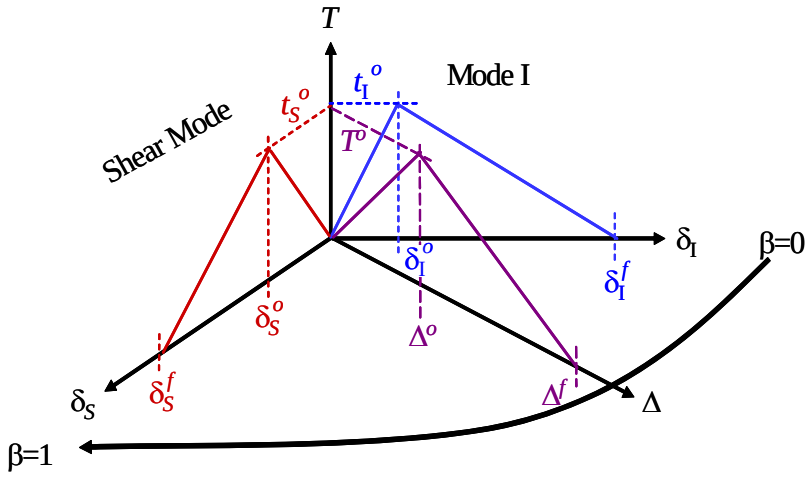

Figure 20. Interpolation of CZM components.

The interpolation of pure mode CZMs shown in Figure 20 is used to develop a mixed mode formulation in Turon et al. (2004). The coupled cohesive zone model is defined by displacement-based onset (Δ^o) and final (Δ^f) criteria. This model uses an interpolation of "normal" and "shear" CZMs to obtain a single coupled CZM for mixed fracture modes. The Mode II and III displacements, δ_{II} and δ_{III}, are combined by the root sum of the squares to make a combined "shear" displacement,

$$\delta_S = \sqrt{(\delta_{\text{II}})^2 + (\delta_{\text{III}})^2} \tag{7}$$

and the coupled displacement across the interface is defined by

$$\Delta = \sqrt{\langle \delta_{\text{I}} \rangle^2 + (\delta_S)^2} \tag{8}$$

where $\langle\ \rangle$ is the MacAuley bracket function, $\langle x \rangle = \frac{1}{2}\left(x + |x|\right)$. Mode mixity parameters are defined by

$$\beta = \frac{\delta_S}{\delta_S + \langle \delta_{\text{I}} \rangle} \qquad\qquad B = \frac{\beta^2}{1 + 2\beta^2 - 2\beta} \tag{9}$$

where $\beta = 0$ for pure Mode I loading, and $\beta = 1$ for pure shear loading. The delamination onset criterion is defined by

$$\Delta^o = \sqrt{(\delta_{\text{I}}^o)^2 + \left[(\delta_S^o)^2 - (\delta_{\text{I}}^o)^2\right] B^\eta} \tag{10}$$

and the final criterion is derived from the B-K critical energy release rate expression (Benzeggagh and Kenane, 1996) given by

$$G_c = G_{\text{Ic}} + (G_{shearc} - G_{\text{Ic}})\left(\frac{G_{shear}}{G_{tot}}\right)^\eta \tag{11}$$

where $G_{tot} = G_{\text{I}} + G_{shear}$, $G_{shear} = G_{\text{II}} + G_{\text{III}}$, and η is an empirical factor used to correlate with experimental data. This leads to an expression for the final opening displacement jump given by

$$\Delta^f = \frac{\delta_{\mathrm{I}}^o \delta_{\mathrm{I}}^f + \left(\delta_S^o \delta_S^f - \delta_{\mathrm{I}}^o \delta_{\mathrm{I}}^f\right) B^\eta}{\Delta^o} \tag{12}$$

In the above expressions, $\delta_{\mathrm{I}}^{\mathrm{f}}$, $\delta_{\mathrm{II}}^{\mathrm{f}}$, and $\delta_{\mathrm{III}}^{\mathrm{f}}$ are the individual modal displacements corresponding to the final criterion and are user-specified. The $\delta_{\mathrm{I}}^{\mathrm{o}}$, $\delta_{\mathrm{II}}^{\mathrm{o}}$, and $\delta_{\mathrm{III}}^{\mathrm{o}}$ are the individual modal displacements corresponding to delamination onset and are computed from the user-specified initial stiffness values, k_{I}^o, k_{II}^o, and k_{III}^o, and peak tractions, t_{I}^o, t_{II}^o, and t_{III}^o, of the CZM. These parameters define the cohesive zone model used in decohesion finite elements for the continuum simulation of fracture at larger length scales.

3.3.1.2 CZM Models for Interfacial Sliding

Cohesive zone models have been used to simulate shear resistance and friction during interfacial sliding, such as grain boundary sliding or sliding between two contact surfaces, in a material. While the process of sliding may look very similar to Mode II or Mode III fracture (as shown in Figure 16), there are several differences between fracture and interfacial sliding, making sliding a fundamentally different deformation mode.

First, by definition, fracture is always related to the creation of a free surface, while in pure sliding (at the atomic scale) there is no free surface creation. For example, during GB sliding, which is a common deformation mechanism in creep deformation (Raj and Ashby, 1971; Yamakov et al., 2002) and governs superplasticity in metals (Ashby and Verrall, 1973), displacement takes place internally between atomic planes and does not require free surface creation.

Second, while fracture is a localized process taking place at a crack tip, sliding is a delocalized process along the entire interface. The associated CZM curve for fracture has a finite displacement jump, and its integration (Eq. 2) always gives a finite energy of decohesion. In contrast, the relative tangential displacement between the two sliding

surfaces (or sliding distance) of an interface has no limit and can be as large as the size of the interface. The tractions (both normal and tangential) do not depend on the displacement but only on the properties of the interface and the applied load. The associated work of friction is proportional to the sliding distance and, unlike the energy of decohesion, is not a property of the interface. The interface dependent property is the friction coefficient, usually defined as the ratio between the tangential and normal tractions $\mu = \tau/\sigma_n$ (Zavattieri and Espinosa, 2003).

Third, fracture creates strong stress gradients due to the stress intensity at the crack tip, while interfacial sliding between smooth surfaces preserves a uniform stress along the sliding planes.

Recently, several CZM models for interfacial sliding have been used. For example, Wei and Anand (2004) modeled the strength of nanocrystalline nickel using CZM models based on experimental data from electrodeposited nanocrystalline Ni. In their model, the Mode I and Mode II cohesive zone curves were very similar, the only difference being that the Mode II curve was extended to twice as large of an opening displacement as Mode I while keeping a relatively small constant stiffness in the plastic region. This resulted in prediction of a certain amount of sliding with some hardening of the Ni grain boundaries before debonding.

Warner et al. (2006) parameterized CZMs for grain boundary sliding in copper using atomistic simulation data. Two major assumptions were made in the parameterization: (i) the shear strength τ_{crit} of the CZM was assumed to be constant with shear displacement, and (ii) the shear and tensile strengths were assumed to be uncoupled because the authors were not able to extract any reliable data on their coupling. Parameterization of CZMs for sliding at contact surfaces that accounts for surface roughness and friction was performed by Zavattieri and Espinosa (2003) for the case of ceramics subjected to pressure-shear loading.

3.3.2 Nanoscopic Length-Scale Coupling Through CZMs

When parameters that are typically used to define the CZMs are taken from bulk material properties (Chen et al., 1999; Iesulauro, 2002; Goyal et al., 2002; Camanho et al., 2003; Zhang and Paulino, 2005), they do not describe the actual physics of microstructural fracture. For metals, macroscale values of strength and toughness that are typically input to the CZM represent the aggregate responses of thousands or millions of grains, grain boundaries, and defects within the specimens from which they were obtained. Thus, these macroscale values do not represent the unique response of a particular interface at which a local fracture event might occur.

If the microscale predictions are to become quantitative, consideration of the local nanoscale properties is required. One means of making this connection is to use the results of atomistic simulation to develop the constitutive relations of CZMs. In this approach, CZM representation of fracture begins at nanometer length scales in which atomistic simulation is used to predict decohesion based on fundamental damage mechanisms. These mechanisms include dislocation formation and interaction, interstitial void formation, and atomic diffusion. The development of these damage mechanisms progress into microscale processes such as local dislocation-based plastic deformation and small crack formation. Ultimately, damage progression leads to macroscopic failure modes such as distributed plastic yielding and the development of large cracks exhibiting Mode I, II, and III opening behavior.

The connection of the CZM constitutive law with, albeit highly idealized, atomistic processes is a starting point for developing more realistic simulations that will eventually lead to accurate predictions of the failure properties of a large class of materials and microstructures, even when experimental data is not available. This methodology constitutes the basis for a sequential multiscale approach to damage modeling.

The first serious attempt to extract relevant parameters for CZM decohesion laws from atomistic (molecular-dynamics or molecular-static) simulations was made by Gall et al. (2000). Here, an atomistic model of an aluminum-silicon interface (Figure 21) was used to study interface debonding. In the simulation, the system was subject to a uniaxial tensile strain normal to the interface until debonding occurred. The internal stress was monitored and plotted as a function of the strain (Figure 22). The extracted atomistic stress-strain curve showed that after an initial elastic stretching, the interface begins to break (at 15% strain), and the stress rapidly decreases and then starts to oscillate around zero due to elastic spring-back effects of the layers after separation. Gall et al., also studied interface debonding for pure aluminum and pure silicon (Figure 23) and found that the Al-Si interface is weaker than either the Al-Al or the Si-Si interface.

It is to be noted, as Gall and co-workers discuss in their paper (Gall et al., 2000), that such atomistically-derived stress-strain relations are not yet applicable for direct extraction of CZM traction-displacement relationships. The atomistic stress-strain plots from these simulations represent the local debonding of an ideal atomically flat interface

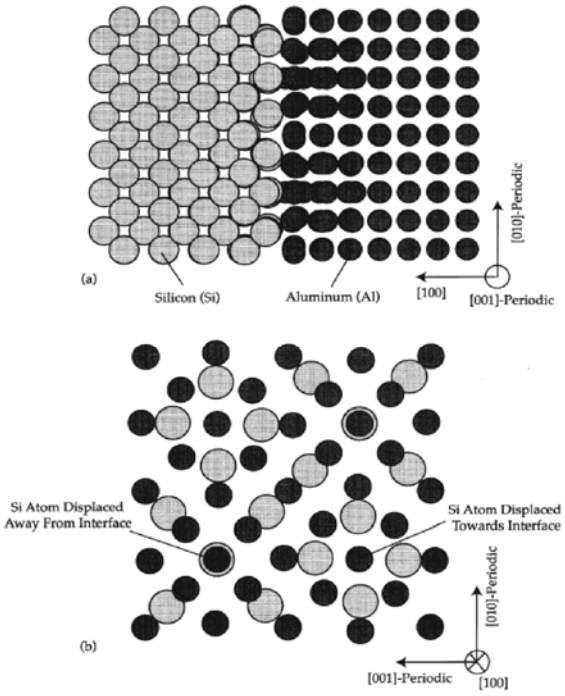

Figure 21. Atomic structure of Al-Si interface. (From Gall et al., 2000)

of dimensions between 10 and 80 nm that does not include the myriad variables that affect the interface. For example, the predicted debonding stress level of ~20 GPa for an Al-Si interface (Figure 23) is highly elevated compared to the experimental ultimate tensile strength of ~200 MPa for a cast Al-Si alloy where fractured and debonded Si particles were observed (Dighe and Gokhale, 1997; Samuel and Samuel, 1995).

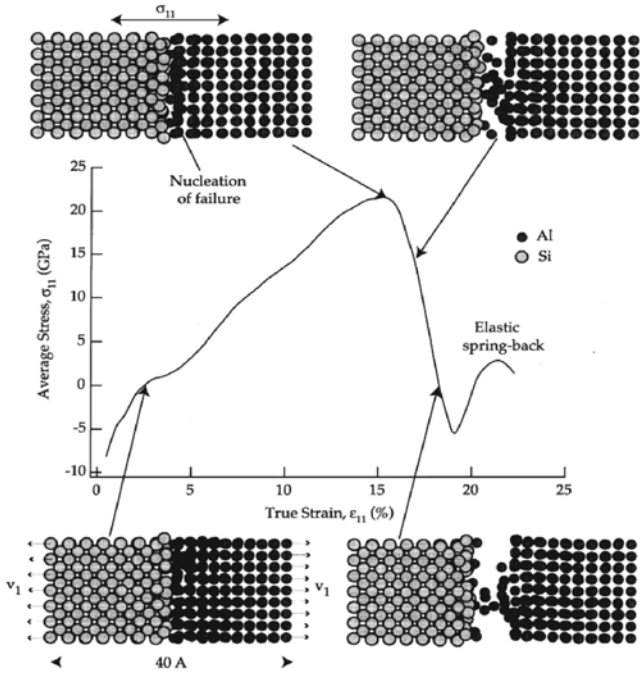

Figure 22. Atomistic derivation of a stress-strain relation during debonding of an Al-Si interface. The four snapshots above and below the plot show structural changes of the interface at different stages of debonding at the atomic level. (From Gall et al., 2000)

Several other attempts to extract relevant parameters for CZM decohesion laws from molecular-dynamics or molecular-static simulations have been made by various groups in the last few years (Komanduri et al., 2001; Spearot et al., 2004). In addition to classical MD simulations, first principles quantum-mechanics based atomistic models (Raynolds et al., 1996) were also used to study adhesion in an NiAl-Cr interface. All of those models showed highly elevated debonding stress ranging from 15 to 50 GPa, which was two orders of magnitude higher than the experimentally observed strength of the corresponding materials.

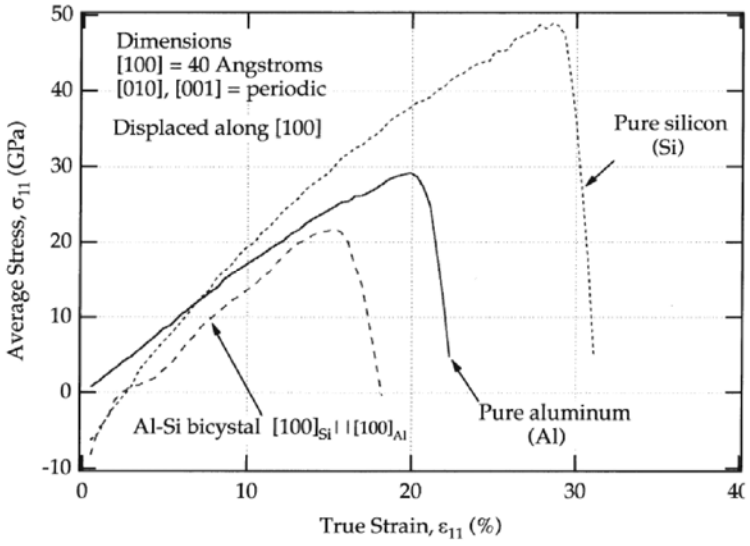

Figure 23. Atomistic stress-strain relations for Al-Si, Al-Al, and Si-Si interfaces. (From Gall et al., 2000)

There are various reasons for this discrepancy between atomistic simulations and experimental characterizations. In addition to various idealizations related to interface structure, an important factor is the selection of ensemble boundary conditions. The approach typically used is based on simulating the debonding of a perfect, flat interface under a constant tensile strain rate perpendicular to the interface. In these references (Komanduri et al., 2001; Spearot et al., 2004; Raynolds et al., 2006), the system size varied between 4 and 80 nm, and the dynamics of the atoms was severely constrained by the boundary conditions, which did not allow for Poisson lateral contraction and shear deformation. In addition, no stress intensity field was generated by introducing an initial crack to simulate a fracture response. As a result, plastic processes, such as dislocation slip, interface sliding, and interface diffusion, were strongly suppressed. Consequently, the simulated mechanism for interface decohesion in these works reproduced an idealized process of atomic adhesion (strength) rather than that of fracture at the interface.

A recent methodology for extracting CZMs from atomistic simulations of crack propagation has been developed to more accurately represent a near-crack tip

configuration (Yamakov et al., 2006). The main goal of this approach was to extract and understand the contributions of different atomistic processes to an MD-based CZM decohesion law for intergranular fracture under local conditions of a propagating crack. The MD model used in this study was built to simulate a crack propagating under steady-state conditions through a flat high-energy grain boundary in aluminum.

A new concept of defining cohesive zone volume elements (CZVE) as an atomistic equivalent of CZM elements was also introduced by Yamakov et al. (2006). In this concept, the CZM is a statistical representation of a large ensemble of CZVEs placed along the crack path during crack propagation (Figure 24). The resulting traction-displacement relationship is obtained as a statistical average of the behavior of a series of CZVEs placed along the crack path during crack propagation. When the propagating crack passes through the CZVEs during the simulation, the resulting stress and opening at each CZVE is determined, and profiles of the stress and opening displacement along the crack are produced (Figure 25). These profiles are taken at 1 ps intervals (time sufficient for a small, but detectable crack advance at the atomic level) during the entire process of crack propagation. The data from the entire set of many such profiles are collected and statistically averaged to produce a CZM traction-displacement relationship (Figure 26) characterizing the overall process of debonding of the interface under study. While the method is still under development, the results to date show the dependence of the CZM law on different plastic processes seen at the atomic scale, such as dislocation nucleation and twinning at the crack tip (Yamakov et al., 2006), heat dissipation (Yamakov et al., 2007), and dynamic fracture processes (Yamakov et al., 2005). While the stress of debonding is still high (~5 GPa) compared to the experimental expectations, the analysis attempts to account for the local conditions of atomic bond breaking at a tip of an atomistically sharp crack and considers a variety of different nanoscale deformation processes inside the crack process zone.

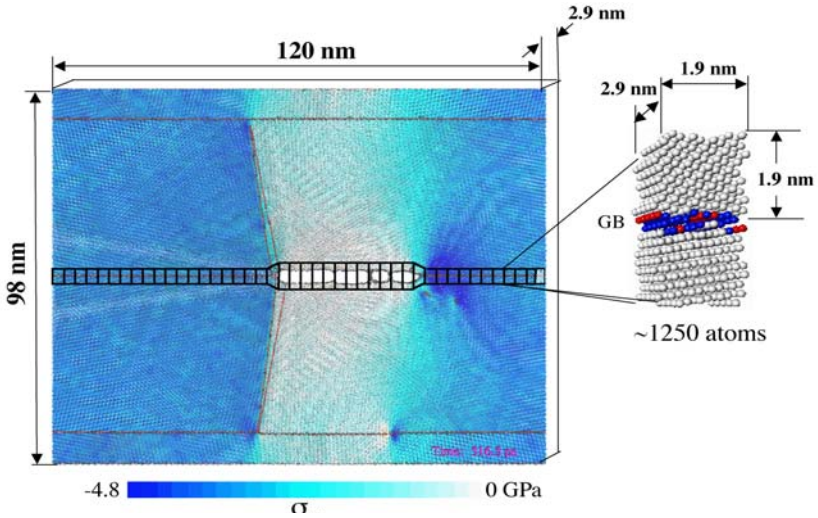

Figure 24. MD simulation of an intergranular crack in aluminum. Cohesive zone volume elements (shown in the inset) are introduced along the grain boundary interface to extract a statistical CZM traction-displacement relationship. (From Yamakov et al., 2006).

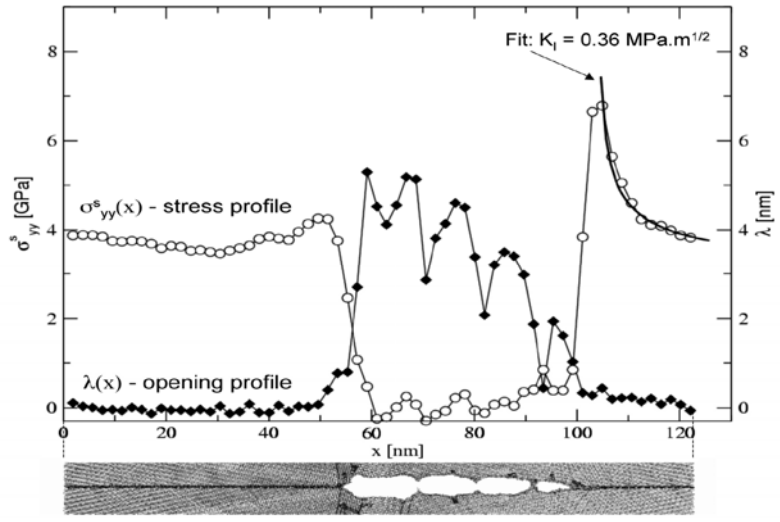

Figure 25. Stress and opening profiles extracted along the crack growing for 123 ps in a system prestressed at 4.25 GPa hydrostatic load. The corresponding snapshot of the crack is shown at the bottom. (From Yamakov et al., 2006).

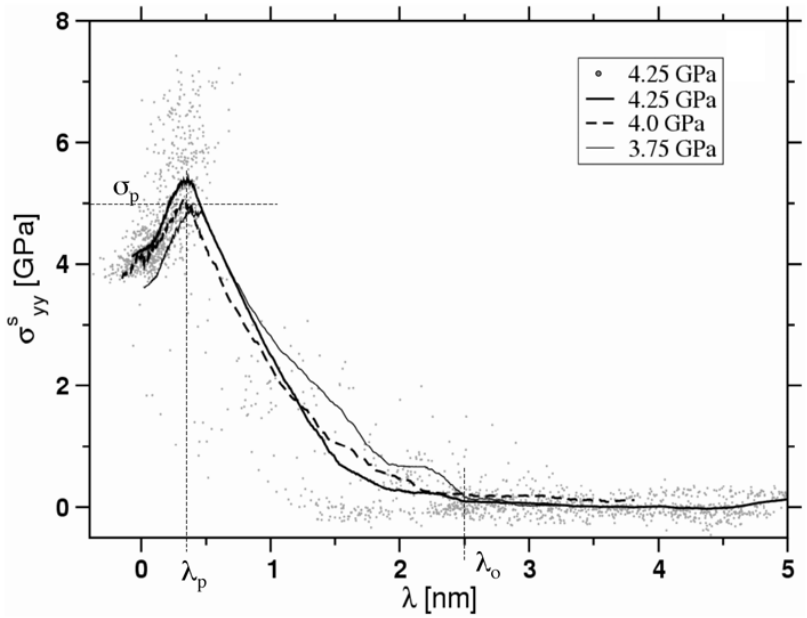

Figure 26. Surface stress vs. crack opening curves $\sigma^s_{yy}(\lambda)$ characterizing the propagation of the cleavage tip for three preloads. (From Yamakov et al., 2006).

3.3.3 Decohesion Finite Element Formulations

Once traction-displacement relationships are known via MD-based analysis or another means, they can be used to define effective decohesion finite elements that can then be placed along potential fracture interfaces in a finite element mesh. The resulting element formulation is referred to herein as a "decohesion" finite element. Finite element simulations can then be used to study failure evolution of material at larger length scales. The methodology is very generic and can be used for any interface that is subjected to fracture, whether the constitutive model is derived at the atomistic scale or determined at a larger length scale.

Decohesion elements are formulated with two sets of coincident nodes defining two superposed surfaces that form a cohesive interface. Shape functions appropriate to the order of assumed variation over the element domain govern the interpolation of quantities over the superposed surfaces. These elements incorporate CZM laws to simulate opening failure modes and are placed between continuum finite elements to

predict softening and ultimate failure of the interface. In fracture studies of metallic materials at the micromechanical level, CZM elements can be used to predict transgranular fracture, if they are placed adaptively between continuum finite elements within grains, or to predict intergranular fracture, if they are placed along grain boundaries as shown in Figure 27.

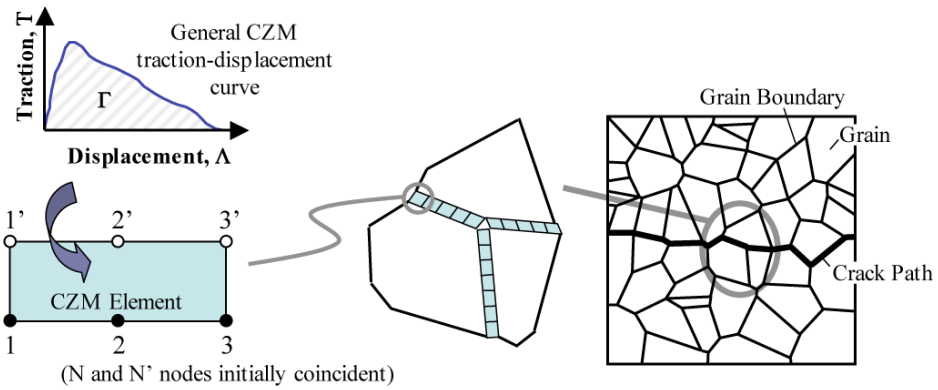

Figure 27. Embedding decohesion elements along GBs to study microstructural fracture.

The decohesion element cohesive surfaces are typically defined as being initially coincident. Figure 28 shows the element surfaces under distortion. In the figure, Ω^+ and Ω^- represent the upper and lower cohesive zone surfaces, respectively. Ω^o represents the interpolated middle surface of the element geometry and is used to define the local element coordinate system.

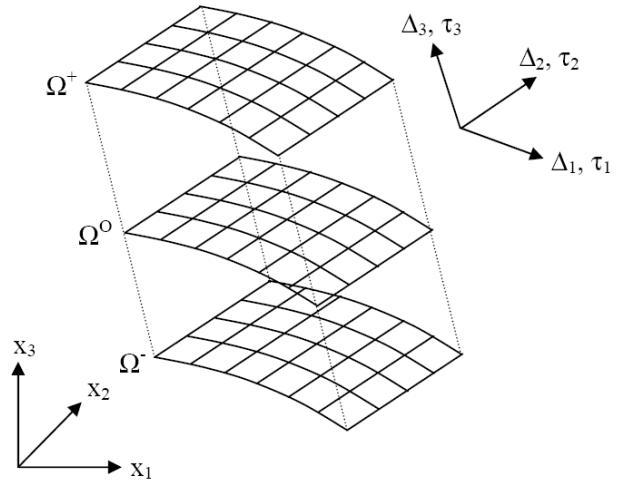

Figure 28. Decohesion finite element configuration.

Examples of decohesion elements are shown in Figures 29 and 30. Figure 29 shows a 1-D 6-node decohesion element configuration. This line element is used to define cohesive interfaces between 2-D continuum elements. Although the element is quadratic, the Mode I opening direction is determined by computing an approximate linear gradient of the relative opening displacements, Δv_i, over the element using only the end nodes. The degree of sliding in Mode II is computed by a summation of all relative displacements, Δu_i, over the element. The kinematics and integration scheme for this element may be found in Alfano and Crisfield (2001).

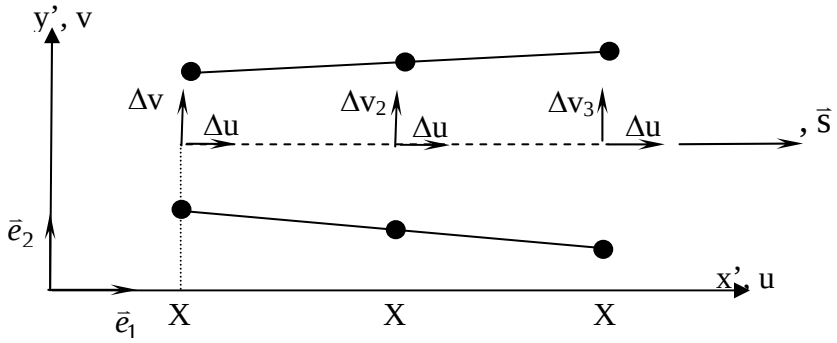

Figure 29. Relative opening displacements for Mode I and Mode II fracture in a 1-D 6-node quadratic decohesion element.

A 2-D 12-node decohesion element is shown in Figure 30. This element is used to define cohesive interfaces between 3-D continuum finite elements. The element is defined with respect to a local (x', y', z') element coordinate system, and the kinematics follow a similar element formulation presented by Segurado and LLorca (2004).

Various aspects of decohesion finite element formulations have been examined in the literature and are briefly summarized here. Convergence difficulties have been encountered and have been related to numerical problems caused by sharp corners in the CZM function during loading and unloading cycles from which large variations in the tangent stiffness matrix can occur (Gao and Bower, 2004). Another effect that can hinder convergence involves the type of numerical quadrature used to evaluate the element integrals. It has been found that Gaussian quadrature tends to link kinematic degrees of

freedom across the element, which affects the eigenmodes of the deformation states, and causes high traction gradients across the element domain. An improvement has been found in using Newton-Cotes methods, which act to uncouple the eigenmodes, thereby resulting in smoother traction profiles and improvement of convergence (Schellekens and de Borst, 1993).

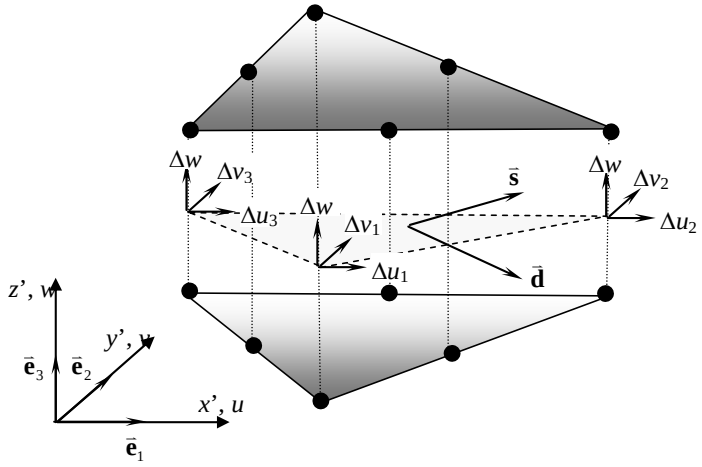

Figure 30. Relative opening displacements for Mode I and Mode II fracture in a 2-D 12-node quadratic decohesion

Additional numerical aspects in the use of decohesion elements exist. To obtain accurate solutions, bounds on element size have been presented (Allen and Searcy, 2000; Tomar et al., 2004; Turon et al., 2007), and augmented solution schemes that include viscous damping to improve convergence characteristics have been advanced (Gao and de Borst, 1993). The initial slope of the traction-displacement law dictates the magnitude of the stiffness penalty constraint and, for macroscopic applications, follows the general rule that this parameter should be chosen large enough to enforce coincidence of nodes at the cohesive surface but not so large as to cause numerical ill-conditioning of the global stiffness matrix. Using a value that is less than optimally-large introduces a spurious compliance into the model that can alter results, particularly in models where decohesion elements are placed between many continuum elements to avoid an a priori assumption of where a dominant crack path will be generated. As the length scale decreases such

that the thickness of the cohesive zone can no longer be assumed infinitesimal, the initial stiffness is no longer a mathematical penalty parameter used to enforce a strict constraint on relative displacements but becomes increasingly reduced to represent the actual elasticity of the finite thickness cohesive zone.

4.0 Summary

This report has presented an overview of the current state of the art for understanding and predicting fracture in polycrystalline metals using principles from the emerging field of nanomechanics. Within this new realm in the study of the mechanics of materials, physics-based modeling of fracture involves the application of molecular dynamics simulation and methods of multiscale analysis. The combination of these computational frameworks, by linking damage mechanisms across length scales, promises future predictions of macroscopic material failure based on fundamental atomistic processes from which all material behavior originates.

Atomistic simulation, often in the form of molecular dynamics, permits a direct simulation of atomistic mechanisms that cause fracture at the nanoscale and that ultimately dictate the overall strength and toughness of a material. These mechanisms include the stretching and breaking of the interatomic bonds and are often accompanied by atomic rearrangements that cause plastic deformation. However, for small submicron material domains requiring a billion atom simulation, the time scale remains severely limited; even the most powerful current supercomputers available today (ca. 2008) can not simulate the system response beyond the nanosecond range. In addition, the very short time scale requires the application of unrealistically high strain rates for atomistic simulations (typically in the range of $10^7 – 10^{12}$ s^{-1}). Therefore, because of their extreme computational expense, molecular dynamics simulation is not well suited to modelling large material domains. This limitation has necessitated the development of multiscale modeling methods to link atomistic simulation within a more computationally efficient framework.

Multiscale modeling methods that join two or more computational paradigms are often characterized as either concurrent or sequential. Concurrent multiscale modeling methods can be used to link molecular dynamics and a continuum mechanics method (e.g., finite element analysis) as a single simultaneously executed analysis. Often, the molecular dynamics simulation is embedded in a much larger finite element analysis. In this application, molecular dynamics is used to determine underlying physical processes and finite element analysis is used to provide appropriate far-field boundary conditions.

Sequential multiscale modeling often uses cohesive zone models to provide the computational bridge between length scales. Cohesive zone models provide a numerically efficient means of representing a broad range of atomic-level mechanisms (i.e. dislocation formation and void formation) and configurations (i.e. grain boundaries) at length scales suitable for continuum mechanics approximations. Typically, the constitutive relationships used in cohesive zone models are approximated using macroscopically derived material properties. However, one new approach for the determination of the cohesive zone models extracts the constitutive relationship from molecular dynamics simulation. This methodology theoretically eliminates empirical descriptions of material degradation by deriving atomistically-based constitutive relations of material strength that can be applied at larger length scales to study the failure of polycrystal microstructures.

The combined methods of molecular dynamic modeling and multiscale analysis techniques permit damage processes to be linked across length scales to ultimately predict macroscopic material behavior from first principles. As analysis methods improve, more realistic simulations will lead to better predictions of the failure properties of a large class of materials and microstructures, even when experimental data is not available or is difficult to obtain.

References

Abraham, F.F., 1997, "On the Transition from Brittle to Plastic Failure in Breaking a Nanocrystal under Tension (NUT)," *Europhys. Lett*. **38**, pp. 103-106.

Abraham, F.F., 2001, "The Atomic Dynamics of Fracture," *J. Mech. Phys. Solids*, **49**, pp. 2095-2111.

Abraham, F.F., Bernstein, N., Broughton, J.Q., and Hess, D., 2000, "Dynamic Fracture of Silicon: Concurrent Simulation of Quantum Electrons, Classical Atoms, and the Continuum Solid," *Materials Research Society Bulletin*, **25**, pp. 27-32.

Abraham, F.F., Walkup, R., Gao, H.J., Duchaineau, M., De la Rubia, T.D., and Seager, M., 2002, "Simulating Materials Failure by Using Up to One Billion Atoms and the World's Fastest Computer Work-Hardening," *Proceedings of the National Academy of Sciences of the United States of America*, **99**, pp. 5783-5787.

Alfano, G. and Crisfield, M.A., 2001, "Finite Element Interface Models for the Delamination Analysis of Laminated Composites: Mechanical and Computational Issues," *Int. J. Num. Meth. Engrg.*, **50**, pp. 1701-1736.

Allan, M.P. and Tildesley, D.J., 1989, *Computer Simulation of Liquids*, Oxford University Press, Oxford, UK.

Allen, D.H. and Searcy, C.R., 2000, "Numerical Aspects of a Micromechanical Model of a Cohesive Zone," *J. Reinforced Plastics and Composites*, **19**, pp. 240-248.

Ashby, M.F. and Verrall, R.A., 1973, "Diffusion-Accommodated Flow and Superplasticity," *Acta Mater*., **21**, pp. 149-163.

Ashurst, W.T. and Hoover, W.G., 1976, "Microscopic Fracture Studies in the Two-Dimensional Lattice," *Phys. Rev. B.*, **14**, pp. 1464-1475.

Barenblatt, G.I., 1959, "The Formation of Equilibrium Cracks During Brittle Fracture. General Ideas and Hypothesis. Axially-Symmetric Cracks," *Prikl. Matem. I mekham*, **23**, pp. 434–444.

Barenblatt, G.I., 1962, "The Mathematical Theory of Equilibrium Cracks in Brittle Fracture," *Adv. Appl. Mech*., **7**, pp. 55-129.

Baskes, M.I., Nelson, J.S., and Wright, A.F., 1989, "Semiempirical Modified Embedded-Atom Potentials for Silicon and Germanium," *Phys. Rev. B.*, **40**, pp. 6085-6100.

Baskes, M.I., 1992, "Modified Embedded-Atom Potential for Cubic Materials and Impurities," *Phys. Rev. B*, **46**, pp. 2727-2742.

Belytschko, T. and Xiao, S.P., 2003, "Coupling Methods for Continuum Model with Molecular Model," *J. Mult. Comput. Engrg.*, **1**, pp. 115-126.

Benzeggagh, M.L. and Kenane, M., 1996, "Measurement of Mixed-Mode Delamination Fracture Toughnesss of Unidirectional Glass/Epoxy Composites with Mixed-Mode Bending Apparatus," *Comp. Sci. and Tech.*, **49**, pp. 439-439.

Born, M. and Huang, K., 1954, *Dynamical Theory of Crystal Lattices*, Oxford University Press, Oxford, UK.

Brenner, D.W., 2000, "The Art and Science of an Analytic Potential," *Phys. Stat. Sol. (b)*, **217**, pp. 23-40.

Broughton, J.Q., Abraham, F.F., Bernstein, N., and Kaxiras, E., 1999, "Concurrent Coupling of Length Scales: Methodology and Application," *Physical Review B*, **60**, pp. 2391-2403.

Buehler, M.J., 2006, "Concurrent Scale Coupling Techniques: From Nano to Macro," Lecture Series 3, CEE, IAP.

Bulatov, V., Abraham, F.F., Kubin, L., Devincre, B., and Yip, S., 1998, "Connecting Atomistic and Mesoscale Simulations of Crystal Plasticity," *Nature*, **391**, pp. 669-672.

Camacho, G.T. and Ortiz, M., 1996, "Computational Modeling of Impact Damage in Brittle Materials," *Int. J. Solids Struct.*, **33**, pp. 2899-2938.

Camanho, P.P., Davila, C.G., and De Moura, M.F., 2003, "Numerical Simulation of Mixed-Mode Progressive Delamination in Composite Materials," *J. Comp. Mat.*, **37**, pp. 1415-1438.

Chandra, N., Li, H., Shet, C., and Ghonem, H., 2002, "Some Issues in the Application of Cohesive Zone Models for Metal-Ceramic Interfaces," *Int. J. Solids Struct.*, **39**, pp. 2827-2855.

Chandra, N., and Shet, C., 2004, "A Micromechanistic Perspective of Cohesive Zone Approach in Modeling Fracture," *CMES: Computer Modeling in Engineering & Sciences*, **5**, pp. 21-33.

Chen, J., Crisfield, M., Kinloch, A.J., Busso, E.P., Matthews, F.L., and Qui, Y., 1999, "Predicting Progressive Delamination of Composite Material Specimens via Interface Elements," *Mech. Comp. Mat. Struct.*, **6**, pp. 301-317.

Clayton, J.D. and Chung, P.W., 2006, "An Atomistic-to-Continuum Framework for Nonlinear Crystal Mechanics Based on Asymptotic Homogenization," *J. Mech. Phys. Solids*, **54**, pp. 1604-1639.

Cleri, F., 2001, "Representation of Mechanical Loads in Molecular Dynamics Simulations," *Phys. Rev. B*, **65**, p. 014107.

Cleri, F., Phillpot, S.R., and Wolf, D., 1999, "Atomistic Simulations of Intergranular Fracture in Symmetric-Tilt Grain Boundaries," *Interface Sci*., **7**, pp. 45-55.

Coble, R.L., 1963, "A Model for Boundary Diffusion Controlled Creep in Polycrystalline Materials," *J. Appl. Phys.*, **34**, pp. 1679-1682.

Costanzo, F. and Allen, D.H., 1995, "A Continuum Thermodynamic Analysis of Cohesive Zone Models," *Int. J. of Engrng. Sci.*, **33**, pp. 2197-2219.

Curtin, W.A. and Miller, R.E., 2003, "Atomistic/Continuum Coupling in Computational Materials Science," *Mod. Sim. Mat. Sci. and Engrg.*, **11,** pp. R33-R68.

Curtin, W.A., 2007, private communication.

Daw, M.S. and Baskes, M.I., 1984, "Embedded-Atom Method: Derivation and Application to Impurities, Surfaces and Other Defects in Metals," *Phys. Rev. B*, **29**, pp. 6443-6453.

DeCelis B, Argon AS, Yip S, 1983, "Molecular Dynamics Simulation of Crack Tip Processes in Alpha-Iron and Copper," *J. App. Phys*., **54**, pp. 4864-4878.

Dighe, M.D. and Gokhale, A.M., 1997, "Relationship Between Microstructural Extremum and Fracture Path in a Cast Al-Si-Mg Alloy," *Scripta Mater.*, **37**, pp. 1435-1440.

Dugdale, D.S., 1960, "Yielding of Steel Sheets Containing Slits," *J. Mech. Phys. Solids*, **8**, pp. 100-108.

Farkas, D., 2000, "Bulk and Intergranular Fracture Behavior of NiAl," *Philos. Mag. A*, **80**, pp. 1425-1444.

Farkas, D., Van Swygenhoven, H., and Derlet, P.M., 2002, "Intergranular Fracture in Nanocrystalline Metals," *Phys. Rev. B*, **66**, pp. 060101-1-4.

Gall, K., Horstemeyer, M.F., Van Schilfgaarde, M., and Baskes, M.I., 2000, "Atomistic Simulations on the Tensile Debonding of an Aluminum-Silicon Interface," *J. Mech. Phys. Solids*, **48**, pp. 2183-2212.

Gao, Y.F. and Bower, A.F., 2004, "A Simple Technique for Avoiding Convergence Problems in Finite Element Simulations of Crack Nucleation and Growth on Cohesive Interfaces," *Mod. Sim. Mater. Sci. Engrg.*, **12**, pp. 453-463.

Glaessgen, E.H., Phillips, D.R., Yamakov, V., and Saether, E., April 19-22, 2005 "Multiscale Modeling for the Analysis of Grain-Scale Fracture Within Aluminum Microstructures," AIAA 2005-1851, 46th AIAA Structures, Structural Dynamics, and Materials Conference, Austin, Texas.

Golubovic, L., Peredera, A., and Golubovic, M., 1995, "Nature of Environmentally Assisted Fracture Nucleation and Crack Growth in Polycrystals," *Phys. Rev. E*, **52**, pp. 4640-4645.

Goyal, V.K., Johnson, E.R., Davila, C.G., and Jaunky, N., 2002, "An Irreversible Constitutive Law for Modeling the Delamination Process Using Interface Elements," NASA/CR-2002-211758.

Grujicic, M., Zhao, H., and Krasko, G.L., 1997, "Atomistic Simulation of Σ3 (111) Grain Boundary Fracture in Tungsten Containing Various Impurities," *Int. J. Refract. Metals Hard Mater*., **15**, pp. 341-355.

Gumbsch, P., 1995, "An Atomistic Study of Brittle-Fracture - Toward Explicit Failure Criteria from Atomistic Modeling," *J. Mat. Res.*, **10,** pp. 2897-2907.

Gumbsch, P., 1999, "Atomistic Modeling of Diffusion-Controlled Interfacial Decohesion," *Mat. Sci. Eng. A*, **260**, pp. 72-79.

Gumbsch, P. and Beltz, G.E., 1995, "On the Continuum Versus Atomistic Descriptions of Dislocation Nucleation and Cleavage in Nickel," *Mod. Sim. Mat. Sci. and Engrg.*, **3,** pp. 597-613.

Hao, S., Liu, W.K., Moran, B., Vernerey, F., and Olson, G.B., 2004, "Multi-Scale Constitutive Model and Computational Framework for the Design of Ultra-High Strength, High Toughness Steels," *Comput. Methods Appl. Mech. Engrg.*, **193**, pp. 1865-1908.

Heino, P., Häkkinen, H., and Kaski, K., 1998, "Molecular-Dynamics Study of Copper with Defects Under Strain," *Phys. Rev. B*, **58**, pp. 641-652.

Hoagland, R.G., 1997, "Crystallographic Aspects of Dislocation Emission from a Crack Tip in an Fcc Metal," *Philos. Mag. A*, **76**, pp. 543-563.

Iesulauro, E., 2002, "Decohesion of Grain Boundaries in Statistical Representations of Aluminum Polycrystals," Cornell University Report 02-01.

Ishida, Y., Mori, M., and Hashimoto, M., 1984, "Molecular Dynamical Calculation of Crack Propagation in Segregated Grain Boundaries of Iron," *Surf. Sci.*, **144**, pp. 253-266.

Johnson, R.A., 1972, "Relationship Between Two-Body Interatomic Potentials in a Lattice Model and Elastic Constants," *Phys. Rev B*, **6**, pp. 2094-2100.

Kem, K.S., McMeeking, R.M., and Johnson, K.I., 1998, "Adhesion, Slip, Cohesive Zones and Energy Fluxes for Elastic Spheres in Contact," *J. Mech. Phys. Solids*, **46**, pp. 243-266.

Klein, P. and Gao, H., 1998, "Crack Nucleation and Growth as Strain Localization in a Virtual-Bond Continuum," *Engr. Fract. Mech*, **61**, pp. 21-48.

Knap, J. and Ortiz, M., 2001, "An Analysis of the Quasicontinuum Method," *J. Mech. Phys. Solids*, **49**, pp. 1899-1923.

Kohlhoff, S., Gumbsch, P., and Fishmeister, H.F., 1991, "Crack Propagation in B.C.C. Crystals Studied with a Combined Finite-Element and Atomistic Model," *Phil. Mag. A*, **64**, pp. 851-878.

Komanduri, R., Chandrasekaran, N., and Raff, L.M., 2001, "Molecular Dynamics (MD) Simulation of Uniaxial Tension of Some Single-Crystal Cubic Metals at Nanolevel," *Int. J. Mech. Sci.*, **43**, pp. 2237-2260.

Kroner, E., 1967, "Elasticity Theory of Materials with Long Range Cohesive Forces," *Int. J. Solids Struct.*, **3**, pp.731-742.

Li, H. and Chandra, N., 2003, "Analysis of Crack Growth and Crack-Tip Plasticity in Ductile Materials Using Cohesive Zone Models," *Int. J.Plast.*, **19**, pp. 849-882.

Li, W. and Siegmund, T., 2004, "Numerical Study of Indentation Delamination of Strongly Bonded Films by use of a Cohesive Zone Model," *CMES: Computer Modeling in Engineering & Sciences*, **5**, pp. 81-90.

Liu, W.K., Karpov, E.G., Zhang, S., and Park, H.S., 2004, "An Introduction to Computational Nanomechanics and Materials," *Comput. Methods Appl. Mech. Engrg.*, **193**, pp. 1529-1578.

Maugis, E., 1992, "Adhesion of Spheres – the JKR-DMT Transition using a Dugdale Model," *J. Colloid Interface Sci.*, **150**, pp. 243-269.

Miller, R.E. and Tadmor, E.B., 2002, "The Quasi-continuum Method: Overview, Applications, and Current Direction," *J. Computer-Aided Materials Design*, **9**, pp. 203-239.

Miller, R., Ortiz, M., Phillips, R., Shenoy, V., and Tadmor, E.B., 1998, "Quasicontinuum Models of Fracture and Plasticity," *Eng. Fract. Mech.*, **61**, pp. 427-444.

Mishin, Y., Farkas, D., Mehl, M.J., and Papaconstantopoulos, D.A., 1999, "Interatomic Potentials for Monoatomic Metals from Experimental Data and Ab Initio Calculations," *Phys. Rev. B*, **59**, pp. 3393-3407.

Mishin, Y., Mehl, M.J., and Papaconstantopoulos, D.A., 2005, "Phase Stability in the Fe-Ni System: Investigation by First-Principles Calculations and Atomistic Simulations," *Acta Mater.*, **53**, pp. 4029-4041.

Needleman, A., 1987, "A Continuum Model for Void Nucleation by Inclusion Debonding," *J. Appld Mech.*, **54**, pp. 525–531.

Needleman, A., 1990a, "An Analysis of Tensile Decohesion along an Interface," *J. Mech. Phys. Solids*, **38**, pp. 289–324.

Needleman, A., 1990b, "An Analysis of Decohesion Along an Imperfect Interface," *Int. J. Fract.*, **42**, pp. 21-40.

Noronha, S.J., Farkas, D., 2002. Dislocation pinning effects on fracture behavior: Atomistic and dislocation dynamics simulations. *Phys. Rev. B*, **66**, 132103-1-4

Nguyen, O. and Ortiz, M., 2002, "Coarse-Graining and Renormalization of Atomistic Binding Relations and Universal Macroscopic Cohesive Behavior," *J. Mech. Phys. Solids*, **50**, pp. 1727-1741.

Oden, J.T., Prudhomme, S., Romkes, A., and Bauman, P., 2006, "Multi-scale Modeling of Physical Phenomena: Adaptive Control of Models," *SIAM Journal on Scientific Computing*, **28**, pp. 2359-2389.

Oden, J.T., Vemaganti, K., and Moes, N., 1999, "Hierarchical Modeling of Heterogeneous Solids," *Comput. Methods Appl. Mech. Engrg.*, **172**, pp. 3-25.

Ohsawa, K. and Kuramoto, E., 1999, "Flexible Boundary Conditions for a Moving Dislocation," *J. Appl. Phys.*, **86**, pp. 179-185.

Ortiz, M. and Pandolfi, A., 1999, "Three-Dimensional Crack Propagation Analysis," *Int. J. Num. Meth. Engrg*, **44**, pp. 1267-1282.

Park, H.S. and Liu, W.K., 2004, "An Introduction and Tutorial on Multiple-Scale Analysis in Solids," *Comput. Methods Appl. Mech. Engrg.*, **193**, pp. 1733-1772.

Raj, R. and Ashby, M.F., 1971, "On Grain Boundary Sliding and Diffusion Creep," *Metall. Trans.*, **2**, p. 1113.

Raynolds, J.E., Smith, J.R., Zhao, G.-L., and Srolovitz, D.J., 1996, "Adhesion in NiAl-Cr from First Principles," *Phys. Rev. B*, **53**, pp. 13883-13890.

Rice, J.R. and Wang, J.-S., 1989, "Embrittlement of Interfaces by Solute Segregation," *Mat. Sci. Engrg. A*, **107**, pp. 23–40.

Rose, J.H, Smith, J.R, and Ferrante, J., 1983, "Universal Feature of Bonding in Metals," *Phys. Rev. B.*, **28**, pp. 1835-1845.

Rudd, R.E. and Belak, J.F., 2002, "Void Nucleation and Associated Plasticity in Dynamic Fracture of Polycrystalline Copper: An Atomistic Simulation," *Comp. Mater. Sci.*, **24**, pp. 148-153.

Rudd, R.E. and Broughton, J.Q., 1998, "Coarse-Grained Molecular Dynamics and the Atomic Limit of Finite Elements," *Phys. Rev. B*, **58**, p. R5893.

Rudd, R.E. and Broughton, J.Q., 2005, "Coarse-Grained Molecular Dynamics: Nonlinear Finite Elements and Finite Temperature," *Phys. Rev. B*, **72**, p. 144104.

Saether, E., Yamakov, V., and Glaessgen, E., April, 2007, "A Statistical Approach for the Concurrent Coupling of Molecular Dynamics and Finite Element Methods," AIAA 2007-

2169, 48th AIAA SDM Structures, Structural Dynamics and Materials Conference, Schaumburg, IL.

Saether, E., Yamakov, V., and Glaessgen, E., 2008, "An Embedded Statistical Method for Coupling Molecular Dynamics and Finite Element Analyses," *Int. J. Num. Meth. Engrg.* (accepted for publication).

Samuel, A. M. and Samuel, F. H., 1995, "A Metallographic Study of Porosity and Fracture Behavior in Relation to the Tensile Properties in 319.2 End Chill Castings," *Metall. Mater. Trans.*, **26A**, pp. 2359-2372.

Schellekens, J.C.J. and de Borst, R., 1993, "On the Numerical Integration of Interface Elements," *Int. J. Num. Meth. Engrg.*, **36**, pp. 43-66.

Segurado, J. and LLorca, J., 2004, "A New Three-Dimensional Interface Finite Element to Simulate Fracture in Composites," *Int. J. Solids and Struct.*, **41**, pp. 2977-2993.

Shen, S. and Atluri, S. N., 2004a, "Computational Nano-Mechanics and Multi-Scale Simulation," *CMC: Computers, Materials, & Continua*, **1**, pp. 59-90.

Shen, S. and Atluri, S. N., 2004b, "Multiscale Simulation Based on the Meshless Local Petrov-Galerkin (MLPG) Method," *CMES: Computer Modeling in Engineering & Sciences*, **5**, pp. 235-255.

Shenoy, V., Shenoy, V., and Phillips, R., 1999, "Finite Temperature Quasicontinuum Methods," *Mater. Res. Soc. Symp. Proc.*, **538**, pp. 465-471.

Shiari, B., Miller, R.E., and Curtin, W.A., 2005, "Coupled Atomistic/Discrete Dislocation Simulations of Nanoindentation at Finite Temperature," *J. Engrg. Mat. and Tech. Transactions of the ASME*, **127,** pp. 358-368.

Shilkrot, L.E., Curtin, W.A., and Miller, R.E., 2002, "A Coupled Atomistic/Continuum Model of Defects in Solids," *J. Mech. and Phys. Solids*, **50**, pp. 2085-2106.

Shilkrot, L.E., Miller, R.E., and Curtin, W.A., 2002, "Coupled Atomistic and Discrete Dislocation Plasticity," *Phys. Rev. Lett.*, **89**, p. 025501.

Shilkrot, L.E., Miller, R.E., and Curtin, W.A., 2004, "Multiscale Plasticity Modeling: Coupled Atomistics and Discrete Dislocation Mechanics," *J. Mech. Phys. Solids*, **52**, pp. 755-787.

Sinclair, J.E., Gehlen, P.C., Hoagland, R.G., and Hirth, J.P., 1978, "Flexible Boundary Conditions and Nonlinear Geometric Effects in Atomistic Dislocation Modeling," *J. Appl. Phys.*, **49**, pp. 3890-3897.

Spearot, D., Jacob, K.I., and McDowell, D.L., 2004, "Non-Local Separation Constitutive Laws for Interfaces and Their Relation to Nanoscale Simulations," *Mech. Mater.*, **36**, pp. 825-847.

Tadmor, E.B., Ortiz, M., and Phillips, R., 1996, "Quasi-continuum Analysis of Defects in Solids," *Phil. Mag. A*, **73**, pp. 1529-1563.

Tadmor, E.B., Phillips, R., and Ortiz, M., 2000, "Hierarchical Modeling in the Mechanics of Materials," *Int. J. Solids & Struct.*, **37**, pp. 379-389.

Tomar, V., Zhai, J., and Zhou, M., 2004, "Bounds for Element Size in a Variable Stiffness Cohesive Finite Element Model," *Int. J. Num. Meth. Engrg.*, **61**, pp. 1894-1920.

Turon, A., Camanho, P.P., Costa, J., and Davila, C.G., 2004, "An Interface Damage Model for the Simulation of Delamination Under Variable-Mode Ratio in Composite Materials," NASA/TM-2004-213277.

Turon, A., Davila, C.G., Camanho, P.P., and Costa, J., 2007, "An Engineering Solution for Mesh Size Effects in the Simulation of Delamination using Cohesive Zone Models," *Eng. Fract. Mech*., **74**, pp. 1665-1682.

Tvergaard, V., 1990, "Effect of Fibre Debonding in a Whisker-Reinforced Metal," *Mat. Sci. and Eng. A*, **125**, pp. 203–213.

Tvergaard, V. and Hutchinson, J. W., 1992, "The Relation Between Crack Growth Resistance and Fracture Process Parameters in Elastic-Plastic Solids," *J. Mech. and Phys. Solids*, **40**, pp. 1377-1397.

Van der Geissen, E. and Needleman, A., 1995, "Discrete Dislocation Plasticity: A Simple Planar Model," *Model. Simul. Mater. Sci. Eng.*, **3**, pp. 689-735.

Voter, A., 1998, "Parallel Replica Method for Dynamics of Infrequent Events," *Phys. Rev. B*, **57**, p. R13985.

Voter, A., Montalenti, F., and Germann, T.C., 2002, "Extending the Time Scale in Atomistic Simulation of Materials," *Annu. Rev. Mater. Res.*, **32**, pp. 321-346.

Wagner, G.J. and Liu, W.K., 2001, "Hierarchical Enrichment for Bridging Scales and Meshfree Boundary Conditions," *Int. J. Num. Meth. Engrg*., **50**, pp. 507–524.

Warner, D.H., Sansoz, F. and Molinari, J.F., 2006, "Atomistic Based Continuum Investigation of Plastic Deformation in Nanocrystalline Copper," *Int. J. Plast.*, **22**, pp. 754-774.

Wei, Y.J. and Anand, L., 2004, "Grain Boundary Sliding and Separation in Polycrystalline Metals: Application to Nanocrystalline FCC Metals," *J. Mech. Phys. Solids*, **52**, pp. 2567-2616.

Wolf, D., 1990, "Correlation Between Structure, Energy, and Ideal Cleavage Fracture for Symmetrical Grain Boundaries in Fcc Metals," *J. Mater. Res.*, **5**, pp. 1708-1730.

Xiao, S.P., and Belytschko, T., 2004, "A Bridging Domain Method for Coupling Continua with Molecular Dynamics," *Comp. Meth. Appld. Mech. Engrg.*, **193**, p.1645.

Xu, X.P. and Needleman, A., 1993, "Void Nucleation by Inclusion Debonding in a Crystal Matrix," *Mod. Sim. Mater. Sci. Engrg.*, **1**, pp. 111–132.

Yamakov, V., Wolf, D., Phillpot, S.R., and Gleiter, H., 2002, "Grain-Boundary Diffusion Creep in Nanocrystalline Palladium by Molecular-Dynamics Simulation," *Acta Mater.*, **50**, pp. 61-73.

Yamakov, V., Saether, E., Phillips, D.R., and Glaessgen, E.H., 2005, "Dynamic Instability in Intergranular Fracture," *Phys. Rev. Lett.*, **95,** p. 015502.

Yamakov, V., Saether, E., Phillips, D.R., and Glaessgen, E.H., 2006, "Molecular-Dynamics Simulation-Based Cohesive Zone Representation of Intergranular Fracture Processes in Aluminum," *J. Mech. Phys. Solids*, **54**, pp. 1899-1928.

Yamakov, V., Saether, E., Phillips, D.R., and Glaessgen, E.H., 2007, "Dynamics of Nanoscale Grain-Boundary Decohesion in Aluminum by Molecular-Dynamics Simulation," *J. Mat. Sci.*, **42**, pp. 1466-1476.

Yip, S. and Wolf, D., 1989, "Atomistic Concepts for Simulation of Grain Boundary Fracture," *Mater. Sci. Forum*, **46**, pp. 77-168.

Zavattieri, P.D., Raghuram, P.V., and Espinosa, H.D., 2001, "A Computational Model of Ceramic Microstructures Subjected to Multi-Axial Dynamic Loading," *J. Mech. Phys. Solids*, **49**, pp. 27-68.

Zavattieri, P.D. and Espinosa, H.D., 2003, "An Examination of the Competition Between Bulk Behavior and Interfacial Behavior of Ceramics Subjected to Dynamic Pressure-Shear Loading," *J. Mech. Phys. Solids*, **51**, pp. 607-635.

Zhang, Z. and Paulino, G.H., 2005, "Cohesive Zone Modeling of Dynamic Failure in Homogeneous and Functionally Graded Materials," *Int. J. Plasticity*, **21**, pp. 1195-1254.

Zhou, S.J., Beazley, D.M., Lomdahl, P.S., and Holian, B.L., 1997, "Large-Scale Molecular Dynamics Simulations of Three-Dimensional Ductile Failure," *Phys. Rev. Lett.*, **78**, pp. 479-482.

REPORT DOCUMENTATION PAGE

Form Approved
OMB No. 0704-0188

1. REPORT DATE *(DD-MM-YYYY)*	2. REPORT TYPE	3. DATES COVERED *(From - To)*
01- 02 - 2009	Technical Memorandum	

4. TITLE AND SUBTITLE

An Overview of the State of the Art in Atomistic and Multiscale Simulation of Fracture

5a. CONTRACT NUMBER

5b. GRANT NUMBER

5c. PROGRAM ELEMENT NUMBER

6. AUTHOR(S)

Saether, Erik; Yamakov, Vasselin; Phillips, Dawn R.; Glaessgen, Edward H.

5d. PROJECT NUMBER

5e. TASK NUMBER

5f. WORK UNIT NUMBER

698259.02.07.07.03.01

7. PERFORMING ORGANIZATION NAME(S) AND ADDRESS(ES)

NASA Langley Research Center
Hampton, VA 23681-2199

8. PERFORMING ORGANIZATION REPORT NUMBER

L-19581

9. SPONSORING/MONITORING AGENCY NAME(S) AND ADDRESS(ES)

National Aeronautics and Space Administration
Washington, DC 20546-0001

10. SPONSOR/MONITOR'S ACRONYM(S)

NASA

11. SPONSOR/MONITOR'S REPORT NUMBER(S)

NASA/TM-2009-215564

12. DISTRIBUTION/AVAILABILITY STATEMENT

Unclassified - Unlimited
Subject Category 26
Availability: NASA CASI (443) 757-5802

13. SUPPLEMENTARY NOTES

14. ABSTRACT

The emerging field of nanomechanics is providing a new focus in the study of the mechanics of materials, particularly in simulating fundamental atomic mechanisms involved in the initiation and evolution of damage. Simulating fundamental material processes using first principles in physics strongly motivates the formulation of computational multiscale methods to link macroscopic failure to the underlying atomic processes from which all material behavior originates. This report gives an overview of the state of the art in applying concurrent and sequential multiscale methods to analyze damage and failure mechanisms across length scales.

15. SUBJECT TERMS

Multiscale analysis; Finite element method; Molecular dynamics; Cohesive zone models; Decohesion finite elements; Polycrystalline metals

16. SECURITY CLASSIFICATION OF:			17. LIMITATION OF ABSTRACT	18. NUMBER OF PAGES	19a. NAME OF RESPONSIBLE PERSON
a. REPORT	b. ABSTRACT	c. THIS PAGE			STI Help Desk (email: help@sti.nasa.gov)
					19b. TELEPHONE NUMBER *(Include area code)*
U	U	U	UU	66	(443) 757-5802